

THICKER SOERGEL CALCULUS IN TYPE A

OR: HOW I LEARNED TO STOP WORRYING AND CALCULATE SOME IDEMPOTENTS

BEN ELIAS

ABSTRACT. Let R be the polynomial ring in n variables, acted on by the symmetric group S_n . Soergel constructed a full monoidal subcategory of R -bimodules which categorifies the Hecke algebra, whose objects are now known as Soergel bimodules. Soergel bimodules can be described as summands of Bott-Samelson bimodules (attached to sequences of simple reflections), or as summands of generalized Bott-Samelson bimodules (attached to sequences of parabolic subgroups). A diagrammatic presentation of the category of Bott-Samelson bimodules was given by the author and Khovanov in previous work. In this paper, we extend it to a presentation of the category of generalized Bott-Samelson bimodules. We also diagrammatically categorify the representations of the Hecke algebra which are induced from trivial representations of parabolic subgroups.

The main tool is an explicit description of the idempotent which picks out a generalized Bott-Samelson bimodule as a summand inside a Bott-Samelson bimodule. This description uses a detailed analysis of the reduced expression graph of the longest element of S_n , and the semi-orientation on this graph given by the higher Bruhat order of Manin and Schechtman.

This paper relies extensively on color figures. Some references to color may not be meaningful in the printed version, and we refer the reader to the online version which includes the color figures.

CONTENTS

1. Introduction	2
2. Background	8
3. Expression graphs and the idempotent	18
4. Thick calculus	44
5. Induced Trivial Representations	51
Appendix A. Summary of notation	55
References	57

1. INTRODUCTION

1.1. Overview. The Hecke algebra \mathbf{H} associated to a Dynkin diagram Γ is an algebra of fundamental importance. Its regular representation can be viewed as the decategorification of the category \mathcal{P} of B -equivariant perverse sheaves on the flag variety, or as the decategorification of the associated category \mathcal{O} , and therefore the Hecke algebra encodes numerics associated to those categories. In the early 90s Soergel provided an additional categorification of the Hecke algebra, known as the category of Soergel Bimodules $\mathbb{S}\text{Bim}$, which is far more accessible than the other two approaches, and can be effectively used to study them both. Soergel bimodules are bimodules over a polynomial ring, and as such, are attractively simple and explicit.

Let us restrict henceforth to finite type A Dynkin diagrams. In [EK10], the author in conjunction with Mikhail Khovanov contributed to this explicit-ness by giving a diagrammatic presentation of $\mathbb{S}\text{Bim}$. More precisely, we gave a diagrammatic presentation of the subcategory $\mathbb{B}\text{SBim} \subset \mathbb{S}\text{Bim}$ of so-called *Bott-Samelson bimodules*. In this description, every morphism can be viewed as a linear combination of planar graphs with boundary (modulo graphical relations), and composition is given by stacking planar graphs on top of each other. For a basic introduction to planar diagrammatics for monoidal categories, we recommend [Lau10, §4]. Planar graphs now provide a simple way to encode what are potentially very complicated maps of bimodules. (More recently, the author and Williamson [EW] have provided a similar diagrammatic calculus for all Coxeter groups.)

This paper continues the elaboration of categorified Hecke theory on several related fronts: by explicitly finding certain important idempotents in $\mathbb{B}\text{SBim}$, by expanding the graphical calculus of [EK10] to the so-called *generalized Bott-Samelson bimodules* $g\mathbb{B}\text{SBim}$, and by giving a diagrammatic presentation of a categorification of induced trivial representations from sub-Dynkin diagrams. Let us define the main players, before we provide some philosophy and motivation.

Let R be the ring of polynomials in n variables, equipped with its action of $W = S_n$. For a subset J of the simple reflections I , which we call a *parabolic subset*, we let R^J denote the subring of R consisting of polynomials invariant under the simple reflections in J . Let B_J be the R -bimodule $B_J := R \otimes_{R^J} R$, so that tensoring with B_J is isomorphic to the functor which restricts an R -module to R^J , and then induces it back to R . When $J = \{i\}$ is a singleton, denote the invariant ring R^i , and let $B_i := R \otimes_{R^i} R$. Tensor products of various B_i are known as *Bott-Samelson bimodules*, and form a full monoidal subcategory $\mathbb{B}\text{SBim}$ of R -bimodules. Similarly, tensor products of B_J are *generalized Bott-Samelson bimodules*, and form a category $g\mathbb{B}\text{SBim}$.

Remark 1.1. Technically, the ring R is graded, and (generalized) Bott-Samelson bimodules are graded R -bimodules which differ from the above by certain grading shifts. We have ignored the grading in this introduction.

The category $\mathbb{S}\text{Bim}$ of *Soergel bimodules* is the full (additive monoidal graded) subcategory of R -bimodules generated by all direct summands of Bott-Samelson bimodules. Soergel has proven [Soe07] that the isomorphism classes of indecomposable Soergel bimodules (up to grading shift) are parametrized by W ; we denote them $\{B_w\}$. The bimodule B_w appears as a summand inside $B_{i_1} \otimes \dots \otimes B_{i_{\ell(w)}}$ for any reduced expression $s_{i_1} \cdots s_{i_{\ell(w)}}$ for w , and does not appear in any “shorter” Bott-Samelson bimodules. Soergel’s proof uses a “support filtration” and is fairly technical. Using this support filtration, one can show that $B_{w_J} = B_J$, where w_J is the longest element of the parabolic subgroup generated by J (see [Wil11]).

Thus B_J will occur as a summand of $B_{i_1} \otimes \dots \otimes B_{i_d}$ whenever $s_{i_1} \cdots s_{i_d}$ is a reduced expression for w_J . There is no known elementary formula for the projection to this summand,

written solely in terms of polynomials. The main result of this paper will be a diagrammatic construction of this projection.

The Grothendieck ring of $\mathbb{S}\text{Bim}$ is isomorphic to the Hecke algebra of S_n . This isomorphism sends the classes $[B_i]$ and $[B_j]$ to the corresponding Kazhdan-Lusztig basis elements. For more details, see [Soe90, Soe92, Soe07].

1.2. Karoubi envelopes and thickening. Describing Soergel bimodules in terms of Bott-Samelson bimodules is an example of a process known as taking the *Karoubi envelope* or the *idempotent completion*. Given an additive category \mathcal{C} , one obtains the Karoubi envelope $\mathbf{Kar}(\mathcal{C})$ (roughly) by adding all direct summands as new objects. In this context, a “direct summand” of an object $M \in \mathcal{C}$ is identified by the idempotent $e \in \text{End}(M)$ which projects to it. Equivalently, if one considers \mathcal{C} as an algebraoid, $\mathbf{Kar}(\mathcal{C})$ is isomorphic to the category of all projective right modules over \mathcal{C} . For more background on the Karoubi envelope, see [BNM06]. In an abstract sense, \mathcal{C} contains all the information necessary to recover $\mathbf{Kar}(\mathcal{C})$, and the two categories are Morita equivalent.

A general philosophy when studying a difficult-to-handle additive category is to study instead an easier, Morita-equivalent subcategory from which the original category can be recovered via the Karoubi envelope. For example, indecomposable Soergel bimodules are difficult to compute with, and the endomorphism algebra of the sum of all indecomposable Soergel bimodules currently defies description except in small cases. However, as noted above, the endomorphism algebra of the sum of all Bott-Samelson bimodules does have a useful description. We mention two other examples of the same phenomenon.

Remark 1.2. In geometric examples, this philosophy typically replaces the study of simple perverse sheaves with the study of pushforwards of constant sheaves from resolutions of singularities.

Example 1.3. Khovanov and Lauda [KL09, KL11] use planar diagrams to present the morphisms between certain semisimple perverse sheaves on quiver varieties (via the work of Varagnolo-Vasserot [VV11]). Rouquier [Rou08] gives the same presentation, without the use of planar diagrams. The Karoubi envelope of this collection of semisimple perverse sheaves contains all perverse sheaves, and thereby categorifies the positive half of the quantum group by work of Lusztig. However, the work of Khovanov-Lauda-Rouquier gives an explicit version of this categorification, and allows for a direct and more general proof of categorification-related results.

Example 1.4. The category of representations of a complex semisimple lie algebra \mathfrak{g} is semisimple, but still difficult to describe as a monoidal category. However, in some cases the subcategory of tensor products of fundamental representations does admit a nice description via planar diagrams. For \mathfrak{sl}_2 , this is the Temperley-Lieb algebra, given its diagrammatic presentation by Kauffman [Kau87]. For rank 2 lie algebras, the corresponding diagrams are the spiders of Kuperberg [Kup96]. Recently in [CKM14], Cautis, Kamnitzer, and Morrison have extended this presentation to type A_n for $n > 2$.

The next step is to translate these successes into results about the interesting category $\mathbf{Kar}(\mathcal{C})$. To study any particular object in $\mathbf{Kar}(\mathcal{C})$, one must be able to realize it as the image of some idempotent in \mathcal{C} . One is led to the following question: given any indecomposable object in $\mathbf{Kar}(\mathcal{C})$, can one find an object $M \in \mathcal{C}$ and an idempotent $e \in \text{End}(M)$ giving rise to it? Usually the object M is obvious from the context, but the idempotent is difficult to compute.

Example 1.5. In the Temperley-Lieb algebra, the idempotents in question are known as Jones-Wenzl projectors, and one has explicit recursive formulas to find them. For \mathfrak{sl}_n the idempotents are called clasps, and there are as yet no formulas for $n > 3$.

Example 1.6. In the Khovanov-Lauda-Rouquier categorification of the positive half of quantum \mathfrak{sl}_2 , the idempotents are easy to find using the technology of Frobenius extensions, see [KL09]. For \mathfrak{sl}_3 the idempotents were uncovered by the wizardry of Stošić [Sto11]. Beyond that nothing is known.

Given a diagrammatic presentation of a category \mathcal{C} , and an idempotent pair (M, e) as above, it is easy to provide a diagrammatic presentation for the category $\mathcal{C}(M, e)$ obtained by formally adjoining the image of e to \mathcal{C} . We discuss this procedure in more depth in §2.4. On the level of morphisms, one adds a projection map $p: M \rightarrow (M, e)$ and an inclusion map $i: (M, e) \rightarrow M$, with the obvious relations $ip = e$ and $pi = \mathbb{1}_{(M, e)}$. Finding e is sufficient to provide a presentation for $\mathcal{C}(M, e)$. Iterating this procedure, one can find a presentation of any *partial idempotent completion* for which one can describe all the idempotents added. Unfortunately, finding idempotents is very difficult in general.

There may be other interesting consequences and formulas involving these new maps: for example, (M, e) may also be a summand of some other object M' , and the inclusion map $(M, e) \rightarrow M'$ may require a computation.

Example 1.7. For Lauda’s categorification [Lau10] of the entire quantum \mathfrak{sl}_2 , a diagrammatic presentation of the Karoubi envelope was given by Khovanov-Lauda-Mackaay-Stošić [KLMS12]. They refer to their new diagrammatics as a “thick calculus,” because the (images of the) new idempotents are represented by thick lines. Their calculus also includes a variety of interesting formulas, such as the Stošić formula.

More generally, one can think of replacing the diagrammatics for \mathcal{C} with the diagrammatics for a partial idempotent completion as *thickening* the calculus; the calculus is not as thick as possible until one adjoins every indecomposable in $\mathbf{Kar}(\mathcal{C})$. One hopes to provide useful formulas to aid computation in a partial idempotent completion, like the Stošić formula.

Let us return to our original context, where $\mathcal{C} = \mathbb{B}\mathbb{S}\mathbf{Bim}$ and $\mathbf{Kar}(\mathcal{C}) = \mathbb{S}\mathbf{Bim}$. Given a reduced expression $w = s_{i_1} \cdots s_{i_d}$ one knows that B_w is a summand inside $B_{i_1} \otimes \cdots \otimes B_{i_d}$, but finding a formula for this idempotent is an incredibly interesting and extremely difficult problem, for which a complete solution is currently out of reach. One should expect that the idempotents may become arbitrarily complex for arbitrary $w \in W$, but that they might be computable for certain classes of $w \in W$.

Remark 1.8. Since the original writing of this paper, the author and Williamson [EW14] have proven the Soergel conjecture, which states that indecomposable Soergel bimodules descend to the Kazhdan-Lusztig basis, when the category is defined over a field of characteristic zero. However, in finite characteristic the sizes of the indecomposable bimodules will change, and so will their images in the Grothendieck group. Finding the idempotents explicitly will tell one which primes need to be inverted for the indecomposable bimodule to have its “generic” size, and can help answer several questions in modular representation theory. As a motivating example, we point the reader to recent work of Williamson [Wil13], who constructs idempotents requiring certain Fibonacci numbers to be invertible, and uses this to disprove the Lusztig conjecture.

In this paper, we compute the idempotents mentioned above for reduced expressions of the longest element w_J in a parabolic subgroup (in type A). In fact, given different reduced

expressions for w_J , we compute the corresponding map $B_{i_1} \otimes \cdots \otimes B_{i_d} \rightarrow B_{i'_1} \otimes \cdots \otimes B_{i'_d}$ which projects to the common summand B_J . This allows one to give a concise and reasonably elegant diagrammatic presentation for the partial idempotent completion $g\mathbb{B}SBim$, a thickening of the original calculus of [EK10].

1.3. Manin-Schechtman theory. To produce the idempotent corresponding to a parabolic subset J , we utilize Manin-Schechtman theory. Manin and Schechtman in [MS89] provide a beautiful and detailed study of a certain n -category associated with the symmetric group S_n . This n -category produces a collection of posets known as the *higher Bruhat orders*, because the most basic such poset is the symmetric group itself with its usual (weak left) Bruhat order.

To describe the next most basic poset, consider the set of all reduced expressions for the longest element $w_0 \in S_n$. This set can be given the structure of a graph by placing an edge between two reduced expressions if they are related by a single braid relation. Manin and Schechtman equip this graph with a specific *semi-orientation*: edges corresponding to the commutation $su = us$ of two commuting simple reflections are unoriented, and called *equivalences*, while edges corresponding to the braid relation $sts = tst$ are oriented. They prove that their directed graph has a unique sink and a unique source up to equivalence. The induced order on equivalence classes of reduced expressions is the first higher Bruhat order.

For the reader's edification, here is a brief description of the higher Bruhat order. Fix the usual total order on the set $X = \{1, \dots, n\}$. Let $P_k(X) = \{I \subset X \text{ such that } I \text{ has size } k\}$, which inherits a lexicographic order. An element $w \in S_n$ can be interpreted as an order on $P_1(X) \cong X$, and its inversion set can be thought of as those $I \in P_2(X)$ such that the induced order on $P_1(I)$ is antilexicographic. The edges in the (weak left) Bruhat graph are induced by the following operation: find $I \in P_2(X)$ such that $P_1(I)$ is an interval in the order, and flip the elements in $P_1(I)$ from lexicographic to antilexicographic. This is the same as multiplying w by a simple reflection on the left. Meanwhile, a reduced expression of w is an order on its inversion set inside $P_2(X)$, saying in which order the inversions were created by simple reflections. For example, the reduced expression sts adds the inversions $\{(12), (13), (23)\}$ in lexicographic order, while tst adds them in antilexicographic order. Now, the higher inversion set of a reduced expression can be thought of as those $I \in P_3(X)$ such that the induced order on $P_2(I)$ is antilexicographic. The higher Bruhat order is induced by the following operation: find $I \in P_3(X)$ such that $P_2(I)$ is an interval in the order, and flip $P_2(I)$ from lexicographic to antilexicographic. There are many interesting subtleties here (such as the equivalence relation) which we sweep under the rug. Ultimately, we will not need the details of their beautiful construction in this paper.

Let $S_m \subset S_n$ be the parabolic subgroup which permutes the subset $\{i+1, \dots, i+m\} \subset \{1, \dots, n\}$. Then there are numerous embeddings of the reduced expression graph for the longest element $w_{0,m}$ of S_m into the reduced expression graph for the longest element $w_{0,n}$ of S_n . There is one embedding for every way to extend $w_{0,m}$ to $w_{0,n}$ by adding simple reflections on the left and right. For example, the graph for $w_{0,3}$ is a single oriented edge, and every oriented edge in the reduced expression graph of $w_{0,n}$ comes from some parabolic embedding $S_3 \subset S_n$. The Manin-Schechtman order is *parabolic compatible* in the sense that these embeddings all preserve orientation (when $\{i+1, \dots, i+m\}$ is also given its usual total order).

Another property of the Manin-Schechtman order is that it is *monoidal* or *local*. Whenever a reduced expression has two braid relations which can be applied in disjoint parts of the expression, there is a corresponding square inside the reduced expression graph, which we call a

disjoint square. The monoidal property states that a disjoint square has a parallel orientation. In other words, whether a given braid relation is to be applied “forwards” or “backwards” is independent of the application of braid relations to distant parts of the expression. That the Manin-Schechtman order is monoidal is to be expected, given that this order is part of a higher n -category.

To any path in a reduced expression graph, we can associate a morphism between the Bott-Samelson bimodules corresponding to the start and end expressions. Equivalences are sent to isomorphisms. However, oriented edges are not sent to isomorphisms. In this paper we focus on the following two properties of the Manin-Schechtman orientation.

- The orientation is *consistent with Bott-Samelson bimodules*, or *BS-consistent*. For oriented paths, the associated morphism does not depend on the oriented path chosen, only on the start and end of the path! The same holds for reverse-oriented paths.
- The orientation on the reduced expression graph for w_0 is *idempotent-magical*. The morphism associated to a path which goes in oriented fashion from source to sink and then in reverse-oriented fashion from sink to source is in fact the idempotent projecting to B_{w_0} ! This property may fail for other elements $w \in S_n$!

The proof that the Manin-Schechtman orientation is BS-consistent goes as follows. For S_4 , BS-consistency is precisely the most interesting relation in the diagrammatic calculus for Bott-Samelson bimodules [EK10], the *Zamolodchikov relation*. Meanwhile, it is proven in [MS89] that the cycles in a reduced expression graph (ignoring cycles which disappear when the non-oriented edges are contracted) are generated by parabolic embeddings of S_4 and by disjoint squares. Thus, BS-consistency follows from being both monoidal and parabolic compatible. The complete proof (dealing with the contracted cycles as well) is given in §3.1.

The Manin-Schechtman orientation is not the only BS-consistent orientation. (We restrict our attention to semi-orientations with a unique source and sink modulo equivalence.) For the longest element of S_4 , there are two such orientations (and their reversals). For S_5 , there are four. Most orientations will not be BS-consistent. As noted in the previous paragraph, whether an orientation is BS-consistent or not is a combinatorial question, pertaining to the disjoint squares and parabolic embeddings of S_4 inside the graph. The combinatorics are rather interesting, and deserve further study.

The idempotent-magical property is very special and quite surprising. This property is also shared by the other BS-consistent orientation for S_4 , and it is unknown whether or not it holds for the other BS-consistent orientations in general. There is currently no understanding for what makes an idempotent-magical orientation special, or why any orientation should have this property to begin with.

The proof that the Manin-Schechtman orientation is idempotent-magical comprises the bulk of this paper, and it is our main technical result. As far as the author is aware, this is the first genuine application of Manin-Schechtman’s orientation (and not just the rough structure of the graph) to representation theory. We use a concrete description of certain oriented paths, and perform very explicit computations to verify the result. The Manin-Schechtman orientation is rather convenient for this. More combinatorial work would be required to prove the result (in the same fashion) for other orientations, though this is theoretically possible.

Remark 1.9. There is a Manin-Schechtman orientation on the reduced expression graphs of arbitrary elements of S_n , not just the longest element. This orientation is always BS-consistent, by the argument above, but is rarely idempotent-magical. For example, there are elements which have only a single equivalence class of reduced expressions, but whose Bott-Samelson bimodules are not indecomposable.

A similar situation seems to occur in type B : I conjecture that one can place a (natural) orientation on the reduced expression graph of the longest element which is parabolic-compatible, monoidal, BS-consistent, and idempotent-magical. This has led the author to conjecture the existence of higher Bruhat orders associated to type B and possibly to other wreath products, and to encourage this study more seriously. Some early work in this direction has recently appeared in [SAV15].

However, the theory appears to break down beyond these cases. A computational result from [EW] shows that the reduced expression graph of the longest element of H_3 does not admit a BS-consistent orientation with a unique source and sink. An unpublished result of the author (essentially, an extremely long exercise) shows that the reduced expression graph of the longest element of D_4 also does not admit a BS-consistent, monoidal orientation! The existence of BS-consistent and idempotent-magical orientations should imply something about the geometry of the flag variety, though what this says about the flag variety in types A and B which fails in type D is a complete mystery. Much more study is required.

Nicolas Libedinsky independently studied a similar question in [Lib11], where he looks at morphisms induced by paths in the expression graph for an arbitrary element $w \in W$, but in the context not of the symmetric group but of *extra large* Coxeter groups ($m_{s,t} > 3$ for any simple reflections s, t). For these Coxeter groups the expression graph is quite simple. Libedinsky shows that the morphism corresponding to any path which hits every reduced expression is an idempotent, and that these idempotents pick out a single isomorphism class of direct summand. However, this summand is typically not indecomposable.

1.4. Singular Soergel bimodules and induced Hecke modules. The entire story of Soergel bimodules should be viewed in the larger context of singular Soergel bimodules, as introduced by Geordie Williamson in his thesis [Wil11]. Singular Soergel bimodules form a 2-category \mathfrak{B} : the objects are rings R^J for each parabolic subset $J \subset \Gamma$, and the Hom categories are some full subcategories of (R^J, R^K) -bimodules. Soergel bimodules form the endomorphism category of the object $R = R^\emptyset$ inside the 2-category of singular Soergel bimodules. The Grothendieck category of \mathfrak{B} is isomorphic to the *Hecke algebroid*, an “idempotent” version of the Hecke algebra. Note that the objects of the Hecke algebroid are also parametrized by parabolic subsets. These results are due to Williamson [Wil11], and more details can be found there.

The *trivial module* of the Hecke algebra is a particular one-dimensional representation. Let T_J denote the induction to \mathbf{H} of the trivial module of the sub-Hecke-algebra \mathbf{H}_J attached to a parabolic subgroup. It is not difficult to show that T_J is isomorphic to $\text{Hom}(J, \emptyset)$ inside the Hecke algebroid, viewed as a module over $\text{Hom}(\emptyset, \emptyset) = \mathbf{H}$. Thus, it is categorified by the singular Soergel bimodule category $\text{Hom}_{\mathfrak{B}}(R^J, R)$.

This paper provides a diagrammatic presentation of $J\text{BSBim}$, the full subcategory of J -singular Bott-Samelson bimodules, which has $\text{Hom}_{\mathfrak{B}}(R^J, R)$ as its idempotent completion. A J -singular Bott-Samelson bimodule is just a usual Bott-Samelson R -bimodule with scalars restricted to R^J on the right. There is a (non-full) faithful functor from $\text{Hom}(R^J, R)$ to $\text{Hom}(R, R) = \text{SBim}$ given by inducing on the right from R^J back up to R . Using the idempotent which picks out B_J , we describe the image of this functor diagrammatically, which allows us to prove that our presentation of $J\text{BSBim}$ is correct. However, the diagrammatic category for $J\text{BSBim}$ is itself quite simple, and can be enjoyed in the absence of any knowledge of the idempotent or its properties, or any knowledge of singular Soergel bimodules.

Finding a diagrammatic presentation of (a Morita-equivalent sub-2-category of) the entire 2-category of singular Soergel bimodules is a more difficult question, and is work in progress

between the author and Williamson. The functor between the description given here of the small fragment $J\mathbb{B}SBim$ and the description in progress of the entire 2-category is straightforward.

Having a categorification of induced trivial modules is a first step towards the categorification of Hecke representation theory in general. Much about the representation theory of the Hecke algebra can be understood using induced trivial and sign modules, and the Hom spaces between them. It is one of the author's goals to categorify this whole picture.

One should also point out that induced modules have been categorified before in much more generality, in the context of category \mathcal{O} , by Stroppel and Mazorchuk [MS08]. It is very likely that the category of this paper should be related to their categorification of the induced trivial module by applying Soergel's functor.

Structure of the paper.

Chapter 2 contains background material. In §2.1 we discuss the Hecke algebra. In §2.2 we elaborate on the Soergel-Williamson categorification, which was partially described in the introduction. In §2.3 we recall the diagrammatic category defined in [EK10], which is equivalent to the category of Bott-Samelson bimodules. Finally, in §2.4 we discuss in detail how partial idempotent completions work, and outline what needs to be computed to thicken our calculus.

In Chapter 3 we perform these computations, and find the idempotent for B_J . In §3.1 we discuss reduced expression graphs and the Manin-Schechtman semi-orientation, and prove that this orientation is BS-consistent. In §3.2 we outline the proof that the orientation is idempotent-magical, and prove it modulo some technical lemmas. The rest of the chapter is a series of awful, terrible computations. In §3.3 we begin the process of proving these technical lemmas, setting notation in place for certain reduced expressions and paths in the reduced expression graph. In §3.4 we describe the extremely important morphism which will become the "thick trivalent vertex." In §3.5 we prove the technical lemmas, and in §3.6 we finish the proof that the idempotent we construct has the desired properties.

In Chapter 4 we use the results of §3 to provide diagrammatics for $g\mathbb{B}SBim$. It should be accessible without reading §3, which the reader uninterested in the specifics is welcome to skip entirely. We augment the diagrammatics by adding new diagrams for interesting morphisms in $g\mathbb{B}SBim$, such as the thick trivalent vertices, and discuss some relations involving these new diagrams.

After all this work, it is quite easy in Chapter 5 to provide diagrammatics for $J\mathbb{B}SBim$, the categorification of the induced trivial module T_J .

The appendix contains a list of notation.

Acknowledgments.

The author was supported by NSF grants DMS-524460 and DMS-524124 and DMS-1103862, and would like to thank Mikhail Khovanov for his suggestions, and Geordie Williamson for many useful discussions. The author also thanks the anonymous referee for many valuable comments, and for pointing out the important missing case (3.22).

2. BACKGROUND

We expect the reader to be familiar with [EK10]. It will be enough to have glanced through Chapters 2 and 3 of that paper; aside from that, we use only once the concept of one-color reduction, found in Chapter 4. Alternatively (perhaps preferably, thanks to the advent of color) one should read [Eli10] chapters 2.1, 2.3 and 2.4. We change the notation for the names of the categories, change the convention for grading shifts, and change the variable t to v

in order to be consistent with more recent papers and the papers of Soergel (wherein, for those who understand, $t = q^{\frac{1}{2}}$ and $v = q^{-\frac{1}{2}}$; in [EK10] we used t for $q^{-\frac{1}{2}}$ in some preliminary versions).

We will not discuss singular Soergel bimodules in this paper. Nonetheless, this additional context may be useful to the reader: we recommend the first three pages of the introduction to [Wil11]. We change notation in that we use the letter b to denote Kazhdan-Lusztig elements, instead of H .

The results below which are attributed to Soergel may be found in [Soe07]. Some of these results appeared in [Soe90, Soe92] first, but [Soe07] has the advantage of being purely algebraic. The results below which are attributed to Williamson may be found in [Wil11]. More information on any of the topics in the first two sections can be found in those papers.

Let us fix some notation pertaining to the symmetric group. Additional notation will be introduced in the various sections of this chapter. We have provided a list of notations in the appendix.

Let $I = \{1, \dots, n\}$ index the vertices of the Dynkin diagram A_n . Elements of I will be called *indices* or *colors*. The terms *distant* and *adjacent* refer to the relative position of two indices in the Dynkin diagram, not in any word or picture. Let $W = S_{n+1}$ be the Coxeter group, with simple reflections s_i , $i \in I$. Let w_0 denote the longest element. For a *parabolic subset* $J \subset I$, let W_J denote its parabolic subgroup. We let w_J be the longest element of W_J , and d_J its length. We say that an index i is *distant* from a parabolic subset J if it is distant from all the indices in J , and we say two parabolic subsets are *distant* if all the indices in one are distant from the indices in the other.

We let $[J]$ denote the Hilbert polynomial of W_J , defined by $v^{-d_J} \sum_{w \in W_J} v^{2l(w)}$. It was denoted $\pi(J)$ in [Wil11]. This Hilbert polynomial is a product of quantum numbers. For instance, the Hilbert polynomial of S_n is $[n]!$, quantum n factorial. Recall that $[n] = v^{-n+1} + v^{-n+3} + \dots + v^{n-3} + v^{n-1}$, and that $[n]! = [n][n-1] \cdots [1]$.

2.1. The Hecke algebra. The Hecke algebra \mathbf{H} has a presentation as an algebra over $\mathbb{Z}[v, v^{-1}]$ with generators b_i , $i \in I$ and the *Hecke relations*

$$\begin{aligned} (2.1) \quad b_i^2 &= (v + v^{-1})b_i \\ (2.2) \quad b_i b_j &= b_j b_i \text{ for distant } i, j \\ (2.3) \quad b_i b_j b_i + b_j &= b_j b_i b_j + b_i \text{ for adjacent } i, j. \end{aligned}$$

The subalgebra \mathbf{H}_J is generated by b_j , $j \in J$. It can also be described by generators and relations in the same way. Note that \mathbf{H} is free over $\mathbb{Z}[v, v^{-1}]$.

There is a basis for \mathbf{H} known as the *Kazhdan-Lusztig basis*, with one element b_w for each $w \in W$. We will not write down this basis explicitly in terms of the generators, nor is it easy to do so. However, we note that when $w = w_J$ is the longest element of a parabolic subgroup, the corresponding basis element $b_J := b_{w_J}$ does have a simple presentation in another basis known as the *standard basis*. When $J = \{i\}$ is a singleton, $b_J = b_i$. When J is empty, $b_\emptyset = 1$.

We will not need any features of the standard basis in this paper, beyond the implications for the Kazhdan-Lusztig basis which we mention in this section.

We also note that b_J is contained inside the subalgebra \mathbf{H}_J . This immediately implies two generalizations of (2.2).

$$(2.4) \quad b_i b_J = b_J b_i \text{ for any } i \text{ distant from } J.$$

$$(2.5) \quad b_J b_K = b_K b_J \text{ for distant } J, K.$$

Working with standard bases, it is also very easy to prove the following, which explains (2.5).

$$(2.6) \quad b_J b_K = b_{J \sqcup K} \text{ for distant } J, K.$$

The Hecke algebra has a *trivial representation* T , a left \mathbf{H} -module. It is free of rank 1 as a $\mathbb{Z}[v, v^{-1}]$ -module, and b_i acts by multiplication by $[2] = v + v^{-1}$. The element b_J acts on T by multiplication by $[J]$, a fact which is obvious when the Hecke algebra is described in terms of the standard basis, see [Wil11, Lemma 2.2.3]. Meanwhile, one knows (see [Lus14, Theorem 6.6]) that $b_i b_w = (v + v^{-1})b_w$ whenever w has s_i in its left descent set. This implies that the $\mathbb{Z}[v, v^{-1}]$ -span of b_K is a realization of the trivial representation of the subalgebra \mathbf{H}_J , whenever $J \subset K$. From this we have the following generalizations of (2.1).

$$(2.7) \quad b_i b_J = b_J b_i = (v + v^{-1})b_J \text{ for any } i \in J$$

$$(2.8) \quad b_J b_K = b_K b_J = [J] b_K \text{ whenever } J \subset K$$

Conversely, any $x \in \mathbf{H}$ for which $b_j x = [2]x$ for all $j \in J$ also satisfies $b_J x = [J]x$, and thus must live in the right ideal of b_J (at least up to scalar). If x is in \mathbf{H}_J as well, then x is a multiple of b_J .

The trivial representation of \mathbf{H} itself is realized inside \mathbf{H} as the span of b_{w_0} , which is also an ideal. A less obvious fact is that the left ideal of b_J is a realization of the induction $T_J := \text{Ind}_{\mathbf{H}_J}^{\mathbf{H}} T$ from the trivial module of \mathbf{H}_J . This also becomes more obvious in the standard basis, see [Wil11].

2.2. The Soergel-Williamson categorification. Let $R = \mathbb{k}[f_1, \dots, f_n]$ be the coordinate ring of the geometric representation of W , where f_i are the simple roots and \mathbb{k} is a field of characteristic $\neq 2$. The ring R is graded with $\deg(f_i) = 2$. If $M = \bigoplus M^i$ is a graded R -module then the grading shift convention will be $M(i)^j = M^{i+j}$. All R -modules in this paper will be graded.

In order to categorify the Hecke algebra within the category of R -bimodules, we may wish to find R -bimodules B_i , $i \in I$, which satisfy

$$(2.9) \quad B_i \otimes B_i \cong B_i(1) \oplus B_i(-1)$$

$$(2.10) \quad B_i \otimes B_j \cong B_j \otimes B_i \text{ for distant } i, j$$

$$(2.11) \quad B_i \otimes B_j \otimes B_i \oplus B_j \cong B_j \otimes B_i \otimes B_j \oplus B_i \text{ for adjacent } i, j.$$

One could then define a map from \mathbf{H} to the split Grothendieck ring of R -bimodules by sending b_i to $[B_i]$. In order to categorify various aspects of the Hecke algebroid, one may also seek R -bimodules B_J for each parabolic set J , which satisfy

$$(2.12) \quad B_J \otimes B_i \cong B_i \otimes B_J \cong B_J(1) \oplus B_J(-1) \text{ whenever } i \in J.$$

$$(2.13) \quad B_J \otimes B_K \cong B_K \otimes B_J \cong [J] B_K \text{ whenever } J \subset K$$

$$(2.14) \quad B_J \otimes B_K \cong B_K \otimes B_J \cong B_{J \sqcup K} \text{ for distant } J, K.$$

Here, we use the shorthand that $[J] B_K$ indicates a direct sum of many copies of B_K with the appropriate degree shifts. The isomorphism (2.12) could be rewritten $B_J \otimes B_i \cong [2] B_J$, for instance. The map from \mathbf{H} to the Grothendieck ring should send b_J to $[B_J]$.

In fact, these modules exist, and we described them briefly in the introduction. Let us recall the construction again. For a more thorough study of this material, see Williamson's thesis [Wil11].

Consider the 2-category (usually called **Bim** in the literature) where the objects are graded rings, and the morphism category between two rings $\text{Hom}(S', S)$ is the category of graded (S, S') -bimodules. Composition of 1-morphisms is given by the tensor product of bimodules. When we write $\text{HOM}(X, Y)$ for X, Y two objects in a graded category, we refer to the graded vector space which is $\bigoplus_{n \in \mathbb{Z}} \text{Hom}(X, Y(n))$. Note that when X, Y are graded (S, S') -bimodules for two commutative rings S, S' , the graded vector space $\text{HOM}(X, Y)$ is also a graded (S, S') -bimodule. We will now describe several 2-subcategories of **Bim**.

The ring R has a natural action of W , and so for each parabolic subset J we have a subring $R^J := R^{W_J}$ of invariants. When $J = \{i\}$ is a single element subset, we abbreviate the invariant ring as R^i . Tensoring on the left with R , viewed as an (R^J, R) -bimodule, is the same as the restriction functor from R -modules to R^J -modules. Tensoring on the left with R , viewed as an (R, R^J) -bimodule, is the same as the induction functor from R^J -modules to R -modules.

Let $B_i := R \otimes_{R^i} R(1)$, which restricts from R down to R^i , and then induces back to R . For a sequence $\underline{i} = i_1 i_2 \dots i_{d(\underline{i})}$ of indices of length $d(\underline{i})$, let $B_{\underline{i}} := B_{i_1} \otimes_R \dots \otimes_R B_{i_{d(\underline{i})}}$. These $B_{\underline{i}}$ are called *Bott-Samelson bimodules*, and together with their grading shifts, form a full monoidal graded subcategory $\mathbb{B}\text{SBim}$ of $\text{Hom}_{\mathbf{Bim}}(R, R)$. Let us mention now that we will write $s_{\underline{i}}$ for the product $s_{i_1} \dots s_{i_{d(\underline{i})}}$, an element of W .

Let $B_J := R \otimes_{R^J} R(d_J)$, which restricts from R down to R^J , and then induces back to R . It is clear that the objects B_J are indecomposable as R -bimodules, being generated by their unique term $1 \otimes 1$ in minimal degree. For a sequence $\underline{J} = J_1 J_2 \dots J_{d(\underline{J})}$ of parabolic subsets, we let $B_{\underline{J}} := B_{J_1} \otimes_R \dots \otimes_R B_{J_{d(\underline{J})}}$. These $B_{\underline{J}}$ are called *generalized Bott-Samelson bimodules*, and together with their grading shifts, also form a full monoidal graded subcategory $g\mathbb{B}\text{SBim}$ of $\text{Hom}_{\mathbf{Bim}}(R, R)$.

The category of *Soergel bimodules* $\mathbb{S}\text{Bim}$ is obtained by taking all direct sums and summands of objects in $\mathbb{B}\text{SBim}$. The objects of $g\mathbb{B}\text{SBim}$ are, in fact, Soergel bimodules. Since Soergel bimodules form an idempotent-closed subcategory of a bimodule category, it has the Krull-Schmidt property and its Grothendieck group will be generated freely by indecomposables. Note that none of the categories mentioned are abelian; *Grothendieck group* always refers to the additive or split Grothendieck group.

It is not hard to see that the bimodules B_i and B_J satisfy the isomorphisms (2.9) through (2.14) above, and we can even be explicit. The isomorphism (2.9) can be deduced from the fact that, as an R^i -bimodule, $R \cong R^i \oplus R^i(-2)$. This isomorphism is given explicitly using the *Demazure operator* $\partial_i: R \rightarrow R^i$, where $\partial_i(P) = \frac{P - s_i(P)}{f_i}$. This operator is R^i -linear, has degree -2, and sends $f_i \mapsto 2$ and $R^i \subset R$ to zero. The two projection operators from R to R^i are $P \mapsto \partial_i(P)$ and $P \mapsto \partial_i(P f_i)$, of degrees -2 and 0 respectively; the inclusion operators are $Q \mapsto \frac{1}{2} f_i Q$ and $Q \mapsto \frac{1}{2} Q$, of degrees +2 and 0 respectively. We invite the reader to figure out the projections and inclusions for (2.9), or to look them up in [EK10]. The Demazure operator also provides an easy way to define the projection and inclusion operators for the splitting in (2.12).

In similar fashion, the isomorphism (2.13) comes from the fact that, as an R^J -bimodule, $R \cong [J] R^J$ up to an overall grading shift. The isomorphism is given explicitly by choosing dual bases for R over R^J with respect to the Demazure operator ∂_{w_J} . More details will be found later, in the discussion before (4.25).

The isomorphism (2.11) was studied closely and made explicit in [EK10].

Consider the isomorphism of (2.14), which is

$$R \otimes_{R^J} R \otimes_{R^K} R(d_J + d_K) = B_J \otimes B_K \cong B_{J \amalg K} = R \otimes_{R^J \amalg R^K} R(d_J + d_K)$$

where J, K are distant. Note that any polynomial in R can be decomposed into polynomials symmetric in either W_J or W_K , so that the left side is spanned by elements $f \otimes 1 \otimes g$ for $f, g \in R$. The isomorphism sends $f \otimes 1 \otimes g \mapsto f \otimes g$.

The following theorem is due to Soergel.

Theorem 2.1. (See [Soe07, Proposition 5.7] or [Wil11, Theorem 4.1.5]) *The Grothendieck ring of $\mathbb{S}Bim$ is isomorphic to \mathbf{H} , where the isomorphism is defined by sending b_i to $[B_i]$ and v to $[R(1)]$. Under this isomorphism, b_J is sent to $[B_J]$. Any Soergel bimodule is free as a left (resp. right) R -module.*

The Hecke algebra is equipped with a canonical $\mathbb{Z}[v, v^{-1}]$ -linear trace map $\varepsilon: \mathbf{H} \rightarrow \mathbb{Z}[v, v^{-1}]$, which picks out the coefficient of 1 in the standard basis of \mathbf{H} . It satisfies $\varepsilon(b_{\mathbf{i}}) = v^{d(\mathbf{i})}$ when \mathbf{i} has no repeated indices, and $\varepsilon(b_J) = v^{d_J}$. The Hecke algebra also has an antilinear antiinvolution ω , satisfying $\omega(v^a b_{\mathbf{i}}) = v^{-a} b_{\omega(\mathbf{i})}$ where $\omega(\mathbf{i})$ is the sequence run in reverse. Together, these induce a pairing on \mathbf{H} via $(x, y) = \varepsilon(y\omega(x))$.

Proposition 2.2. (See [Soe07] Theorem 5.15) *This canonical pairing is induced by the categorification $\mathbb{S}Bim$, in that the graded rank of $\text{HOM}_{\mathbb{S}Bim}(X, Y)$ as a free left (or right) R -module is precisely $([X], [Y])$.*

Putting together the previous theorems, we can state the following useful lemma, which tells us when an idempotent in $\text{End}(B_{\mathbf{i}})$ will pick out B_J .

Lemma 2.3. *Let X be a summand of $B_{\mathbf{i}}$ for some reduced expression \mathbf{i} of w_J . Suppose that X satisfies $X \otimes B_i \cong X(1) \oplus X(-1)$ for all $i \in J$. Then the class of X in \mathbf{H} is a scalar multiple of b_J , and this scalar is the graded rank of the free R -module $\text{HOM}(R, X)$, divided by v^{d_J} . In particular, if $\text{HOM}(R, X)$ and $\text{HOM}(R, B_J)$ have the same graded rank, then $X \cong B_J$.*

Proof. Whatever $[X]$ is, it is contained in \mathbf{H}_J and satisfies $[X]b_i = (v + v^{-1})[X]$, so $[X]$ must actually be a scalar multiple of b_J (as discussed in §2.1). Since $\text{HOM}(R, X)$ has graded rank $\varepsilon([X])$ and $\varepsilon(b_J) = v^{d_J}$, we can determine the scalar from this graded rank by dividing by v^{d_J} . If $[X] = b_J$ then by computing the graded rank of $\text{END}(X)$ we know that X is indecomposable, and it must therefore be isomorphic to B_J . \square

There is one more category to describe, in order to categorify the induced trivial module T_J in a combinatorial way. Let $J\mathbb{S}Bim$, the category of J -singular Bott-Samelson bimodules, denote the full subcategory of (R, R^J) -bimodules given by objects $\text{Res}B_{\mathbf{i}}$, where the Bott-Samelson bimodule $B_{\mathbf{i}}$ is restricted to become an R^J -module on the right. These are special examples of singular Soergel bimodules, as described in the introduction. Williamson has generalized the results of Soergel above to singular Soergel bimodules [Wil11]. To avoid needing to discuss singular Soergel bimodules in this paper, we only sketch a proof the following claim.

Claim 2.4. *The idempotent completion of $J\mathbb{S}Bim$ is the category of singular Soergel bimodules inside (R, R^J) -bimodules. In particular, $J\mathbb{S}Bim$ categorifies T_J .*

Proof. Using the classification theorem of indecomposable singular Soergel bimodules (see [Wil11, Theorem 5.4.2]) we know there is one indecomposable for each coset of W_J in W . Let $s_{\mathbf{i}}$ be a reduced expression for the minimal element w of that coset, and consider the restriction of $B_{\mathbf{i}}$. Using the support filtration (see [Wil11]), it is clear that this restriction has the indecomposable corresponding to that coset appearing as a summand with multiplicity 1. (Thanks to Williamson for this quick proof.)

That this is a categorification of T_J comes from [Wil11, Theorem 4.1.5]. \square

The remaining facts about $J\mathbb{B}SBim$ that we will use can be quoted directly from [Wil11, Theorems 4.1.5 and 5.2.2].

Claim 2.5. *Morphism spaces between two objects in $J\mathbb{B}SBim$ are free as left R -modules and right R^J -modules. There is a formula for the graded ranks of HOM spaces in $J\mathbb{B}SBim$, analogous to the Proposition above for Soergel bimodules.*

The functor which induces from R^J to R on the right is fully faithful after base change. That is, for $X, Y \in J\mathbb{B}SBim$ we have

$$\text{HOM}_{(R,R)}(X \otimes_{R^J} R, Y \otimes_{R^J} R) \cong \text{HOM}_{(R,R^J)}(X, Y) \otimes_{R^J} R.$$

We will provide diagrammatics for the category $J\mathbb{B}SBim$ in Chapter 5.

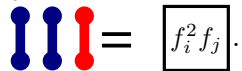
2.3. Soergel diagrammatics. In [EK10], the author and M. Khovanov give a diagrammatic presentation of a category \mathcal{D} by generators and relations. A functor $\mathcal{F}: \mathcal{D} \rightarrow \mathbb{B}SBim$ was constructed, and it was shown that \mathcal{F} is an equivalence when the base field \mathbb{k} is of characteristic not equal to 2.

Technically, morphisms in \mathcal{D} are graded vector spaces, which describe the space $\text{HOM}(X, Y)$ between two Bott-Samelson bimodules. We write Hom spaces in \mathcal{D} as $\text{HOM}_{\mathcal{D}}(X, Y)$ accordingly. Obtaining a graded category, whose morphisms all have degree 0, is a trivial process. We will also ignore the difference between \mathcal{D} and its additive closure, speaking freely about direct sums of objects in \mathcal{D} .

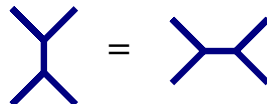
What follows is a brief summary of sections 2.3 and 2.4 of [Eli10]. If this is the reader's first encounter with Soergel diagrammatics, we recommend reading those sections instead, as a better introduction. We will assume that many of the ideas found there are known to the reader, including biadjointness, dot forcing rules, idempotent decompositions, and one-color reductions. One can also see [EK10] for a less pretty version, but a version where the equivalence \mathcal{F} between \mathcal{D} and $\mathbb{B}SBim$ is explicitly defined.

An object in the diagrammatic version of $\mathbb{B}SBim$ is given by a sequence of indices \underline{i} , which is visualized as d points on the real line \mathbb{R} , labelled or "colored" by the indices in order from left to right. Morphisms from \underline{i} to \underline{j} are planar graphs in $\mathbb{R} \times [0, 1]$, with each edge colored by an index, with bottom boundary \underline{i} and top boundary \underline{j} . The allowed vertices are univalent vertices (degree +1), trivalent vertices joining 3 edges of the same color (degree -1), 4-valent vertices joining edges of alternating distant colors (degree 0), and 6-valent vertices joining edges of alternating adjacent colors (degree 0).

We will occasionally use a shorthand to represent double dots (two univalent vertices connected by an edge). We identify a double dot colored i with the polynomial $f_i \in R$, and to a linear combination of disjoint unions of double dots in the same region of a graph, we associate the appropriate linear combination of products of f_i . For any polynomial $f \in R$, a square box with a polynomial f in a region will represent the corresponding linear combination of graphs with double dots. We have a bimodule action of R on morphisms by placing boxes (i.e. double dots) in the leftmost or rightmost regions of a graph. The functor \mathcal{F} respects this R -bimodule action.

For instance, .

In the following relations, blue represents a generic index.

(2.15) 

$$(2.16) \quad \begin{array}{c} \diagup \\ \diagdown \end{array} = | = \begin{array}{c} \diagdown \\ \diagup \end{array}$$

$$(2.17) \quad \bigcirc = 0$$

$$(2.18) \quad \begin{array}{c} \bullet \\ | \\ \bullet \end{array} + \begin{array}{c} | \\ \bullet \\ | \\ \bullet \end{array} = 2 \begin{array}{c} \bullet \\ | \\ \bullet \end{array}$$

We have the following implication of (2.18):

$$(2.19) \quad || = \frac{1}{2} \left(\begin{array}{c} \bullet \\ \diagup \\ \diagdown \\ \bullet \end{array} + \begin{array}{c} \diagdown \\ \diagup \\ \bullet \end{array} \right).$$

In the following relations, the two colors are distant.

$$(2.20) \quad \begin{array}{c} \diagdown \\ \diagup \end{array} = ||$$

$$(2.21) \quad \begin{array}{c} \diagdown \\ \diagup \end{array} = \begin{array}{c} \diagdown \\ \bullet \\ \diagup \end{array}$$

$$(2.22) \quad \begin{array}{c} \diagdown \\ \diagup \end{array} = \begin{array}{c} \diagdown \\ \diagup \\ \bullet \end{array}$$

$$(2.23) \quad \begin{array}{c} \bullet \\ | \\ \bullet \end{array} = \begin{array}{c} | \\ \bullet \\ | \\ \bullet \end{array}$$

In this relation, two colors are adjacent, and both distant to the third color.

$$(2.24) \quad \begin{array}{c} \diagdown \\ \diagup \end{array} = \begin{array}{c} \diagdown \\ \diagup \end{array}$$

In this relation, all three colors are mutually distant.

$$(2.25) \quad \begin{array}{c} \diagdown \\ \diagup \end{array} = \begin{array}{c} \diagdown \\ \diagup \end{array}$$

Remark 2.6. Relations (2.20) thru (2.25) indicate that any part of the graph colored i and any part of the graph colored j “do not interact” for i and j distant. That is, one may visualize sliding the j -colored part past the i -colored part, and it will not change the morphism. We call this the *distant sliding property*.

In the following relations, the two colors are adjacent.

$$(2.26) \quad \begin{array}{c} \diagdown \\ \diagup \end{array} = \begin{array}{c} \diagdown \\ \bullet \\ \diagup \end{array} + \begin{array}{c} \diagdown \\ \diagup \end{array}$$

$$(2.27) \quad \begin{array}{c} \text{Three vertical lines (left blue, middle red, right blue)} \\ = \\ \text{A red loop with blue lines crossing it} - \text{A blue Y-junction with red lines} \end{array}$$

$$(2.28) \quad \begin{array}{c} \text{A blue Y-junction with red lines} \\ = \\ \text{A red Y-junction with blue lines} \end{array}$$

$$(2.29) \quad \begin{array}{c} \text{A red dot on a blue line} - \text{A blue dot on a red line} \\ = \\ \text{A blue dot on a blue line} - \text{A red dot on a red line} \end{array}$$

We have the following implication of the above:

$$(2.30) \quad \begin{array}{c} \text{A blue Y-junction with red lines} \\ = \\ \text{A red loop with blue lines crossing it} \end{array}$$

In this final relation, the colors have the same adjacency as $\{1, 2, 3\}$.

$$(2.31) \quad \begin{array}{c} \text{A complex 6-valent vertex with blue, red, and green lines} \\ = \\ \text{A complex 6-valent vertex with blue, red, and green lines in a different configuration} \end{array}$$

Theorem 2.7 (Main Theorem of [EK10]). *There is a functor \mathcal{F} from \mathcal{D} to $\mathbb{B}S\text{Bim}$, which is an equivalence of categories. Thus, the indecomposable objects in $\mathbf{Kar}(\mathcal{D})$ are parametrized by $w \in W$.*

We will abusively call these indecomposable objects B_w , even though that is their image under the functor \mathcal{F} , because denoting them w would be even more confusing notation.

You can start paying attention again NOW.

We do not recall the definition of \mathcal{F} because it is largely irrelevant. Let $1 \otimes 1 \otimes \dots \otimes 1 \in B_{\underline{i}}$ be called a *1-tensor*. It will be significant that the 6-valent vertex and the 4-valent vertex both send 1-tensors to 1-tensors. So does the dot, positioned so that it represents a map from $B_i \rightarrow R$, and the trivalent vertex, positioned so that it represents a map from $B_i \rightarrow B_i \otimes B_i$. When the trivalent vertex is positioned so that it represents a map from $B_i \otimes B_i \rightarrow B_i$, the corresponding map of bimodules will simply apply the Demazure operator ∂_i to the middle term in $R \otimes_{R^i} R \otimes_{R^i} R$.

The relation (2.27) is sent under \mathcal{F} to the first direct sum decomposition below, while flipping the colors yields the second. Here, blue is i , red is $i + 1$, and $J = \{i, i + 1\}$.

$$(2.32) \quad B_i \otimes B_{i+1} \otimes B_i = B_J \oplus B_i$$

$$(2.33) \quad B_{i+1} \otimes B_i \otimes B_{i+1} = B_J \oplus B_{i+1}.$$

That is, the identity $1_{i(i+1)i}$ is decomposed into orthogonal idempotents. The first idempotent, which we call a *doubled 6-valent vertex*, is the projection from $B_i \otimes B_{i+1} \otimes B_i$ to its

summand B_J . The 6-valent vertex itself is the projection from $B_i \otimes B_{i+1} \otimes B_i$ to B_J and then the inclusion into $B_{i+1} \otimes B_i \otimes B_{i+1}$.

We call the following map, which is the projection from $i(i+1)i$ to the “wrong” summand, by the name *aborted 6-valent vertex*.

$$(2.34) \quad \begin{array}{c} \diagup \quad \diagdown \\ | \\ \text{red dot} \end{array}$$

Because projections to different summands are orthogonal, we have the following key equation, a simple consequence of (2.26), (2.15) and (2.17):

$$(2.35) \quad \begin{array}{c} \text{blue circle} \\ \diagup \quad \diagdown \\ | \\ \text{red dot} \end{array} = 0$$

Several times in this paper we will use the fact that the morphism

$$(2.36) \quad \begin{array}{c} \text{blue H} \\ | \\ \text{red dot} \end{array}$$

factors through the aborted 6-valent vertex. This follows from (2.15).

2.4. Thickening. In this section, we discuss in detail some general facts about partial idempotent completions. We will eventually use the observations of this chapter to enhance the diagrammatics \mathcal{D} for $\mathbb{B}\mathcal{S}\mathcal{B}\text{im}$ above into a diagrammatic calculus $g\mathcal{D}$ for $g\mathbb{B}\mathcal{S}\mathcal{B}\text{im}$.

Definition 2.8. Let \mathcal{C} be a full subcategory of an ambient module category. By assuming this, we guarantee that the idempotent completion is fairly nice (Krull-Schmidt); in particular, it is also embedded in the same ambient category. If \mathcal{S} is a set of objects in the idempotent completion of \mathcal{C} , we let $\mathcal{C}(\mathcal{S})$ be the full subcategory of the ambient module category whose objects are those of \mathcal{C} as well as \mathcal{S} . We call this a *partial idempotent completion* or a *thickening* of \mathcal{C} . When \mathcal{S} consists of a single object M , we denote the thickening by $\mathcal{C}(M)$.

Let us assume that we have a description of all morphisms in \mathcal{C} , by generators and relations, and that M is a module in the idempotent completion. We may pick out M by using a particular idempotent φ_X inside some object $X \in \mathcal{C}$ of which M is a summand.

Claim 2.9. *To obtain a presentation of $\mathcal{C}(M)$ by generators and relations, we may take as generators the generators of \mathcal{C} along with two new maps $p_X: X \rightarrow M$ and $i_X: M \rightarrow X$, and as relations the relations of \mathcal{C} along with $i_X p_X = \varphi_X$ and $p_X i_X = \mathbb{1}_M$.*

Proof. This is a tautological fact about idempotent completions, which we spell out this once. By definition, $\text{Hom}_{\mathcal{C}(M)}(M, Y) = \text{Hom}_{\mathcal{C}}(X, Y)\varphi_X$, that is, those morphisms $X \rightarrow Y$ which are unchanged under precomposition by φ_X . The map i_X corresponds to $\varphi_X \in \text{End}(X)$ itself, and in the thickening, all maps from $M \rightarrow Y$ will clearly be compositions of i_X with some map $X \rightarrow Y$. Similar dual statements may be made about p_X and maps to M . Therefore i_X, p_X are the only new generators required. Any relations among maps factoring through M arise from relations for maps factoring through X (by definition of morphisms in $\mathcal{C}(M)$) and these can all be deduced using the relations stated above. \square

While this is sufficient to describe $\mathcal{C}(M)$, the result is not necessarily an intuitive description. The object M may have a variety of interesting maps to various objects in \mathcal{C} , whose properties could be deduced solely from the properties of φ_X , but which are not obvious *a priori*. For instance, it is not even obvious which other objects Y might have M as a summand.

One thing we can do is augment our presentation (or diagrammatics) by adding new symbols for certain maps which can be constructed out of maps in \mathcal{C} and the new maps p_X, i_X . That is, we add a new generator paired with a new relation which defines the new generator in terms of the existent morphisms. We can then deduce some relations which hold among these new symbols, by checking them in $\mathcal{C}(M)$. In doing so, one need not worry about the eternal questions one faces when given a presentation: do we have enough relations? Do we have too many? We already have a presentation, and we are merely adding new symbols and relations as a more intuitive shorthand.

One useful such augmentation will be to produce inclusions and projections for other objects Y of which M is a direct summand, using only the maps i_X, p_X and maps in \mathcal{C} .

Claim 2.10. *Given a summand M of X defined by idempotent φ_X , M will also be a summand of Y if and only if there exist maps $\varphi_{X,Y}: X \rightarrow Y$ and $\varphi_{Y,X}: Y \rightarrow X$ such that $\varphi_{X,Y}\varphi_X = \varphi_{X,Y}$, $\varphi_X\varphi_{Y,X} = \varphi_{Y,X}$, and $\varphi_{Y,X}\varphi_{X,Y} = \varphi_X$.*

Proof. We let the inclusion map $i_Y: M \rightarrow Y$ be $i_Y := \varphi_{X,Y}i_X$, and similarly we define the projection $p_Y := p_X\varphi_{Y,X}$. Conversely, given inclusion and projection maps to Y , we let $\varphi_{X,Y} = i_Y p_X$ and $\varphi_{Y,X} = i_X p_Y$. The reader may verify that this works. \square

Thus, if we know what the transition maps $\varphi_{X,Y}$ are explicitly, then we may augment our presentation by adding new maps i_Y and p_Y , and relations as in the claim above and its proof. Having such an augmentation will make it more obvious that M is a summand of both Y and X . The point is that the data of the transition maps is data which is entirely defined in terms of morphisms in \mathcal{C} , not in any completion thereof.

We now generalize this to the form we will use, and leave proofs to the reader. In the claim below, one should think of $\varphi_{X,X}$ as the idempotent φ_X .

Claim 2.11. *Suppose that we have a nonempty collection $\{X_\alpha\}$ of objects in \mathcal{C} for which M is a summand (that is, with each object we fix an inclusion and projection map defining M as a summand). Let $\varphi_{\alpha,\beta}$ be the map $X_\alpha \rightarrow X_\beta$ given by the composition $X_\alpha \rightarrow M \rightarrow X_\beta$ of a projection map with an inclusion map. Note that this implies $\varphi_{\beta,\gamma}\varphi_{\alpha,\beta} = \varphi_{\alpha,\gamma}$. The maps $\varphi_{\alpha,\beta}$ are morphisms in \mathcal{C} , so let us suppose that we know how to describe these maps explicitly. We may obtain a presentation of $\mathcal{C}(M)$ as follows. The generators will consist of those generators of \mathcal{C} as well as new maps $p_\alpha: X_\alpha \rightarrow M$ and $i_\alpha: M \rightarrow X_\alpha$. The relations will consist of those relations in \mathcal{C} as well as the new relations $i_\beta p_\alpha = \varphi_{\alpha,\beta}$ and $p_\alpha i_\alpha = \mathbb{1}_M$.*

Claim 2.12. *A collection of functions $\varphi_{\alpha,\beta}: X_\alpha \rightarrow X_\beta$ will define a mutual summand if and only if $\varphi_{\beta,\gamma}\varphi_{\alpha,\beta} = \varphi_{\alpha,\gamma}$ for all α, β, γ .*

Definition 2.13. We call a collection of morphisms $\varphi_{\alpha,\beta}$ satisfying $\varphi_{\beta,\gamma}\varphi_{\alpha,\beta} = \varphi_{\alpha,\gamma}$ a *consistent family of projectors*.

Remark 2.14. A similar concept is a *consistent family of isomorphisms*, which occurs when all $\varphi_{\alpha,\beta}$ are isomorphisms. This is the data required to state that a family of objects are canonically isomorphic. In fact, the idempotent $\varphi_{\alpha,\alpha}$ will produce an object of the Karoubi envelope for each α , and the maps $\varphi_{\alpha,\beta}$ will descend to a consistent family of isomorphisms between these various objects.

This concludes the discussion of adding numerous projections and inclusions to the presentation of $\mathcal{C}(M)$. Of course, we may want to augment our presentation still further, to help describe other features of the new objects.

Remark 2.15. Given a consistent family of projectors, a map in $\mathcal{C}(M)$ from M to any object Z can be specified by one of the following equivalent pieces of data

- for a single X of which M is a summand, a map f from $X \rightarrow Z$ such that $f\varphi_{X,X} = f$,
- a “consistent” family of maps $f_\alpha: X_\alpha \rightarrow Z$ such that $f_\alpha\varphi_{\beta,\alpha} = f_\beta$.

We will usually define a map by using one member of the consistent family, but once the map is defined, we will freely use any member of the family (and will often investigate what certain other members of the family look like).

Note that we can also let g be an arbitrary map $X \rightarrow Z$, without assuming that $g\varphi_{X,X} = g$, and let $f = g\varphi_{X,X}$. Then f will yield a map from M to Z . In this description, multiple different maps g can give rise to the same map f , so the description is not unique.

The goal of the next chapter is to present $g\mathbb{B}\mathbb{S}\mathbb{B}\text{im}$ by generators and relations. We know that, for any parabolic subgroup J , B_J will be a summand of $B_{\underline{i}}$ where \underline{i} is any reduced expression for w_J . For instance, $B_{s_1s_2s_1s_3s_2s_1}$ is a summand of $B_{s_1} \otimes B_{s_2} \otimes B_{s_1} \otimes B_{s_3} \otimes B_{s_2} \otimes B_{s_1}$. The set of reduced expressions for w_J gives a family of objects in $\mathbb{B}\mathbb{S}\mathbb{B}\text{im}$ for which we wish to have inclusion and projection maps, which means that we will need to find an explicit description of a consistent family of projectors $\varphi_{\underline{i},\underline{j}}: B_{\underline{i}} \rightarrow B_{\underline{j}}$ for any two reduced expressions of w_J .

Proposition 2.16. *Suppose that one has a family of maps $\varphi_J = \{\varphi_{\underline{i},\underline{j}}\}$ for each pair of reduced expressions of w_J , which satisfy the following three properties.*

- *The family φ_J is a consistent family of projectors, picking out a summand X .*
- *The summand X satisfies $X \otimes i \cong X(1) \oplus X(-1)$ for each $i \in J$.*
- *The space $\text{HOM}_{\mathcal{D}}(X, \emptyset)$ is a cyclic R -module, generated in degree $+d_J$.*

Then X is indecomposable, and is sent by the functor \mathcal{F} to the Soergel bimodule B_J .

Proof. This follows immediately from Lemma 2.3. □

Finding these maps φ_J and proving these three properties is the job of the next chapter.

3. EXPRESSION GRAPHS AND THE IDEMPOTENT

3.1. Expression graphs and path morphisms. Most of the terminology of this section is ad hoc, but there does not seem to be any standard terminology in the literature.

Definition 3.1. Let w be an element of S_n . Let $\widetilde{\Gamma}_w$, the *expanded expression graph*, be the set of reduced expressions for w . We give $\widetilde{\Gamma}_w$ the structure of an undirected graph by placing an edge between x and y if and only if they are related by a single application of either $s_i s_j s_i = s_j s_i s_j$ for i, j adjacent, or $s_i s_j = s_j s_i$ for i, j distant. We may distinguish between these two different kinds of edges, calling the former *adjacent edges* and the latter *distant edges*. Distant edges will be drawn as dashed lines in the examples below.

We may shorten reduced expressions to a sequence of indices, such as 121 for $s_1 s_2 s_1$.

We may place an orientation on the adjacent edges of the expanded expression graph, using the *lexicographic partial order*, so that arrows always go from $i(i+1)i$ to $(i+1)i(i+1)$. The distant edges remain unoriented. When we speak of an *oriented path* in $\widetilde{\Gamma}$, we refer to a path which may follow distant edges freely, but can only follow adjacent edges along the orientation. A *reverse oriented path* is an oriented path backwards. When we say *path* with no specification, we refer to any path, which may follow the adjacent edges in either direction.

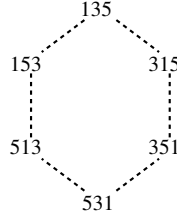
Example 3.2. The expanded expression graph for 21232 in S_4 .

$$12312 \quad \cdots \cdots \cdots \quad 12132 \quad \longrightarrow \quad 21232 \quad \longrightarrow \quad 21323 \quad \cdots \cdots \cdots \quad 23123$$

Definition 3.3. Let Γ_w , the (*conflated*) *expression graph*, be the graph which is the quotient of $\tilde{\Gamma}$ by all distant edges; that is, one identifies any two vertices connected by a distant edge, and removes the distant edges.

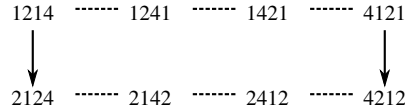
The following examples will include some important definitions.

Example 3.4. The expanded expression graph for 135 in S_6 .



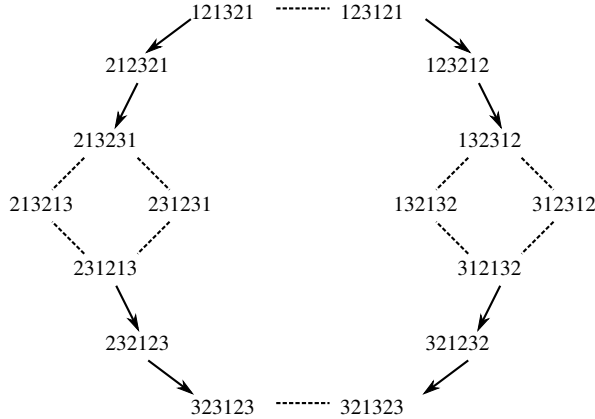
There are two distinct paths from 135 to 531, which form a hexagon. We refer to any cycle of this form appearing in any expanded expression graph (which will occur whenever $\dots ijk \dots$ occurs inside a larger word, for i, j, k all mutually distant) as a *distant hexagon*. Note that the conflated expression graph is a point.

Example 3.5. The expanded expression graph for 1214 in S_5 .



There are two distinct (oriented) paths from 1214 to 4212, which form an octagon. As above, we refer to any cycle of this form in any expanded expression graph as a *distant octagon*. Note that the conflated expression graph is a single edge.

Example 3.6. The expanded expression graph for the longest element 121321 in S_4 .



There are different kinds of cycles appearing here. For instance, a square is formed between 213231 and 231213, because there are two *disjoint* distant moves which can be applied, and one can apply them in either order. Any square of this kind in any graph we call a *disjoint square*. A disjoint square can involve distant or adjacent edges, with parallel edges having the same type. For example, there is a disjoint square or adjacent edges from 121343 to 212434.

Ignoring the ambiguities created by the two disjoint squares in this picture, or considering the conflated expression graph, there are two oriented paths from 121321 to 323123. We refer to any cycle of this form in any expanded expression graph as a *Zamolodchikov cycle*.

Expression graphs were studied deeply in Manin-Schechtman [MS89]. In that paper they define an n -category, where one can at various stages view expressions as objects, distant and adjacent edges as morphisms between objects, the cycles above as 2-morphisms between morphisms, and on to even higher structure. We will use only a few of their results here.

Remark 3.7. To the casual reader, it may not be obvious how Manin-Schechtman discusses expression graphs at all in [MS89], or how the results there translate into the results here. We recommend closely reading §2 of that paper just for the example of $I = \{1, \dots, n\}$ and $k \leq 4$, and skimming §3, always keeping the examples of S_3 (see Chapter 3 Example 6) and S_4 in mind. The key results will be Theorem 3 and Lemma/Corollary 8 from §2, which we will translate below.

Proposition 3.8. *For any $w \in S_n$, the graph $\widetilde{\Gamma}_w$ is connected. The 4 types of cycles mentioned above (disjoint squares, distant hexagons, distant octagons, and Zamolodchikov cycles) generate $H^1(\widetilde{\Gamma}_w)$ topologically. Viewing these cycles as transformations on oriented paths (switching locally from one oriented path in a cycle to the other), any two oriented paths with the same source and target can be reached from each other by these cycles.*

The same statements are true for Γ_w , restricting oneself only to disjoint squares and Zamolodchikov cycles (for the remaining cycles are trivial in Γ_w).

Proof. See [MS89, §2, Corollary 8]. In fact, the disjoint squares and Zamolodchikov cycles in Γ_w essentially give rise to the two different kinds of edges in the next higher Bruhat order. \square

Now we see how to combine the theory of expression graphs with morphisms in \mathcal{D} .

Definition 3.9. To a vertex $\mathbf{x} \in \widetilde{\Gamma}_w$ we may associate an object $B_{\mathbf{x}} \in \mathcal{D}$, which is simply the sequence of indices corresponding to \mathbf{x} . (Although $B_{\mathbf{x}}$ looks more like an object in $\mathbb{B}S\text{Bim}$, we felt this made it easier to distinguish between the vertex in $\widetilde{\Gamma}$ and the corresponding object in \mathcal{D} .) To a path $\mathbf{x} \rightsquigarrow \mathbf{y}$ in $\widetilde{\Gamma}_w$ we may associate a morphism $B_{\mathbf{x}} \rightarrow B_{\mathbf{y}}$ in \mathcal{D} , by assigning the 4-valent vertex to a distant edge, and the 6-valent vertex to an adjacent edge. We call this the *path morphism* associated to the path. To a length 0 path at vertex $B_{\mathbf{x}}$ we associate the identity morphism of $B_{\mathbf{x}}$. Note that reversing the direction of a path will correspond to placing the path morphism upside-down.

We will consistently use bold letters for vertices in $\widetilde{\Gamma}_w$ or Γ_w . The notation $B_{\mathbf{x}}$ is just like the notation $B_{\mathbf{i}}$, and in fact \mathbf{x} is a special kind of sequence \mathbf{i} .

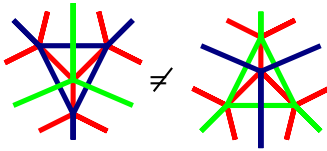
Proposition 3.10. *Let f and g represent two oriented (resp. reverse oriented) paths from \mathbf{x} to \mathbf{y} . Then their path morphisms are equal. In the notation of the introduction, this orientation is BS-consistent.*

Proof. Since oriented paths f and g are related by the various cycle transformations above (in Proposition 3.8) we need only show that the path morphism is unchanged under these cycle transformations. Because \mathcal{D} is a monoidal category, the morphisms associated to either path in a disjoint square are equal. Relation (2.25) is a restatement of the fact that the morphisms associated to either path in the distant hexagon are equal; similarly for (2.24) and the distant octagon. Relation (2.31) is a restatement of the fact that the morphisms associated to either *oriented* path in the Zamolodchikov cycle are the same. Flipping the pictures upside-down yields the statement for reverse oriented paths. There is one additional kind of loop which is possible for oriented paths: following a distant edge from \mathbf{x} to \mathbf{y} and then right back to \mathbf{x} . But this is the identity by (2.20). \square

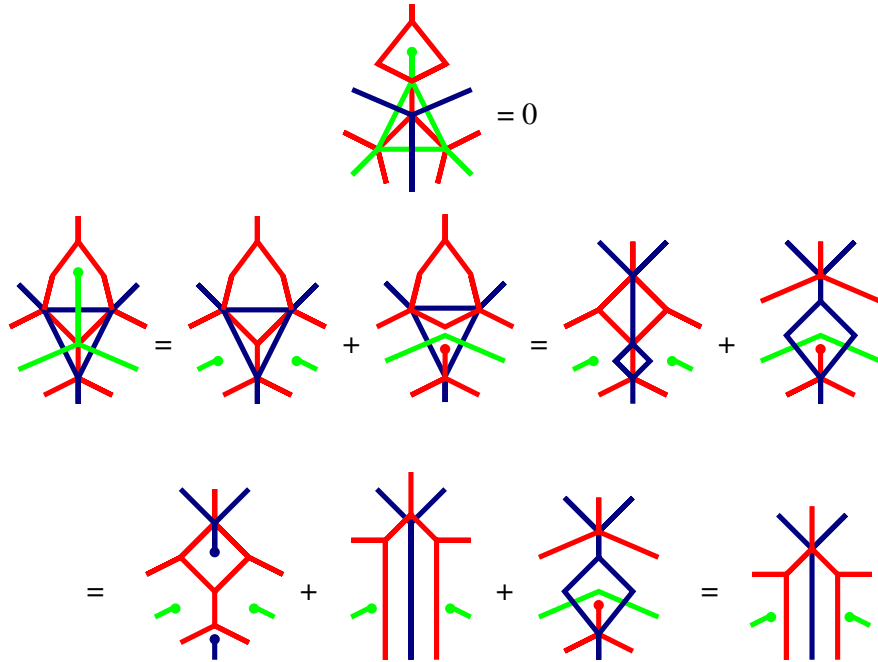
Remark 3.11. If \mathbf{x} and \mathbf{y} are connected by a distant edge, then the loop $B_{\mathbf{x}} \rightarrow B_{\mathbf{y}} \rightarrow B_{\mathbf{x}}$ is the identity of $B_{\mathbf{x}}$, while if the edge is an adjacent edge then the loop is *not* the identity, but is instead the doubled 6-valent vertex, an idempotent of $B_{\mathbf{x}}$. In this sense adjacent edges and distant edges are unsurprisingly different.

Remark 3.12. In the Zamolodchikov cycle for the longest element of S_4 , some of the non-oriented paths are non-equal (beyond the trivial example of the previous remark).

For instance, consider the two possible (necessarily unoriented) path morphisms from 212321 to 321232 which don't recross an oriented edge. These are pictured below as morphisms fitting in a circle with boundary 212321232123, and where blue, red, and green represent 1, 2, 3 respectively.

(3.1) 

To show that they are non-equal, we attach an aborted 6-valent vertex to the top of both sides: the right is clearly zero by (2.35), while the left is nonzero.



In this calculation, the first equality comes from (2.26), the second from (2.28) and (2.30), the third from (2.27), and the fourth from (2.35).

Corollary 3.13. *Consider a set of vertices $\{\mathbf{x}_\alpha\}$ which are connected using only distant edges, and let $\varphi_{\alpha,\beta}$ be the (unique) path morphism (using only distant edges) from $B_{\mathbf{x}_\alpha}$ to $B_{\mathbf{x}_\beta}$. Then φ forms a consistent family of isomorphisms.*

Proof. Because the paths use only distant edges, they are oriented, and their compositions are also oriented. The previous proposition therefore immediately implies that $\varphi_{\beta,\gamma}\varphi_{\alpha,\beta} = \varphi_{\alpha,\gamma}$. They are isomorphisms since $\varphi_{\alpha,\alpha}$ is the identity map. \square

The 4-valent vertices/distant edges are all isomorphisms and do not play a significant role. Henceforth, whenever we speak of the *length* of a path in $\widetilde{\Gamma}_w$ we mean the number of adjacent edges in the path (i.e. the length in Γ_w).

Definition 3.14. We abuse notation henceforth in order to talk about path morphisms of Γ instead of $\widetilde{\Gamma}$. To a vertex $\mathbf{x} \in \Gamma$ we may associate a class of objects, one for each vertex in $\widetilde{\Gamma}$ lifting \mathbf{x} , with a fixed family of transition isomorphisms between them. To a path $\mathbf{x} \rightsquigarrow \mathbf{y}$ in Γ , we may associate its *path morphism*, by which refer to the family of morphisms from some lift of \mathbf{x} to some lift of \mathbf{y} given by some lift of the path, or equivalently, to any specific morphism in this family. See Remark 2.15.

3.2. Statement, outline, and preliminaries. We now restrict our attention to the graph $\Gamma = \Gamma_{w_0}$ for the longest element of S_{n+1} .

Notation 3.15. Suppose that $\mathbf{x} \rightarrow \mathbf{y}$ is an edge in Γ . We write $\mathbf{x} \downarrow \mathbf{y}$ to denote the unique length 1 oriented path from \mathbf{x} to \mathbf{y} , which is just the edge. We write $\mathbf{y} \uparrow \mathbf{x}$ for the reverse-oriented length 1 path from \mathbf{y} to \mathbf{x} .

Meanwhile, for $\mathbf{x}, \mathbf{y} \in \Gamma$, we write $\mathbf{x} \searrow \mathbf{y}$ for some oriented path from \mathbf{x} to \mathbf{y} of unspecified length, assuming that one exists. We write $\mathbf{y} \nearrow \mathbf{x}$ for some reverse-oriented path. We write $\psi_{\mathbf{x} \searrow \mathbf{y}}$ and $\psi_{\mathbf{y} \nearrow \mathbf{x}}$ for the corresponding path morphisms, which do not depend on the choice of oriented path by Proposition 3.10.

For any path V , we write \overline{V} for the reversed path. For any diagram D in \mathcal{D} , we write \overline{D} for the same diagram flipped upside-down. If D is the path morphism of V , then \overline{D} is the path morphism of \overline{V} .

Proposition 3.16. *There is a unique source \mathbf{s} in Γ , and a unique sink \mathbf{t} . Let m be the length of the shortest (not necessarily oriented) path from \mathbf{s} to \mathbf{t} . Then every vertex lies on some oriented path $\mathbf{s} \searrow \mathbf{t}$ of length m , and every oriented path $\mathbf{x} \searrow \mathbf{y}$ can be extended to a length m path $\mathbf{s} \searrow \mathbf{x} \searrow \mathbf{y} \searrow \mathbf{t}$.*

Proof. See [MS89, §2, Theorem 3]. In fact, for the longest element of S_{n+1} , one has $m = \binom{n+1}{3}$. \square

It is easy to see what \mathbf{s} and \mathbf{t} are: we give a representative vertex in $\widetilde{\Gamma}$ for the vertex in Γ .

- $n = 1$: $\mathbf{s} = 1$, $\mathbf{t} = 1$.
- $n = 2$: $\mathbf{s} = \underline{121}$, $\mathbf{t} = \underline{212}$.
- $n = 3$: $\mathbf{s} = 121\underline{321}$, $\mathbf{t} = 323\underline{123}$.
- $n = 4$: $\mathbf{s} = 121321\underline{4321}$, $\mathbf{t} = 434234\underline{1234}$.
- $n = 5$: $\mathbf{s} = 1213214321\underline{54321}$, $\mathbf{t} = 5453452345\underline{12345}$.

At each stage, for \mathbf{s} , we add a new sequence $n, n-1, \dots, 1$. The reader should be able to see the pattern.

Definition 3.17. For $\mathbf{x}, \mathbf{y} \in \Gamma$, let $\varphi_{\mathbf{x}, \mathbf{y}} = \psi_{\mathbf{x} \searrow \mathbf{y}} \circ \psi_{\mathbf{t} \nearrow \mathbf{s}} \circ \psi_{\mathbf{x} \searrow \mathbf{t}}$. In other words, $\varphi_{\mathbf{x}, \mathbf{y}}$ is corresponds to any path which goes from \mathbf{x} down to the bottom, up to the top, and then down to \mathbf{y} . Let $\chi_{\mathbf{x}, \mathbf{y}} = \psi_{\mathbf{t} \nearrow \mathbf{y}} \circ \psi_{\mathbf{s} \searrow \mathbf{t}} \circ \psi_{\mathbf{x} \nearrow \mathbf{s}}$ correspond to the any path which goes from \mathbf{x} up to the top, down to the bottom, and then up to \mathbf{y} .

Note that we have described a family of morphisms for vertices in Γ instead of $\widetilde{\Gamma}$, but the two concepts are functionally equivalent via Definition 3.14.

Our main theorem, constructing the idempotent for the longest element, is the following.

Theorem 3.18. *One has $\varphi_{\mathbf{x},\mathbf{y}} = \chi_{\mathbf{x},\mathbf{y}}$ for all $\mathbf{x}, \mathbf{y} \in \Gamma$. The family φ is a consistent family of projectors. Its image is the indecomposable object B_{w_0} corresponding to the longest element.*

If instead we had worked with Γ_{w_J} for the longest element of W_J , where J is a connected parabolic subset (so that $W_J \cong S_m$ for some m), we would obtain the indecomposable object B_J corresponding to w_J .

In the remainder of this section, we give an outline of the proof of Theorem 3.18. We also discuss the part of the proof which just manipulates paths in Γ , without needing to perform any calculations involving path morphisms.

Definition 3.19. Let $Z = \psi_{\mathbf{s} \searrow \mathbf{t}}$ denote the unique oriented path morphism from source to sink. Let $\bar{Z} = \psi_{\mathbf{t} \nearrow \mathbf{s}}$ denote the unique reverse-oriented path morphism from sink to source.

Note that $\varphi_{\mathbf{t},\mathbf{s}} = \bar{Z}$, $\chi_{\mathbf{s},\mathbf{t}} = Z$, and $\varphi_{\mathbf{s},\mathbf{s}} = \chi_{\mathbf{s},\mathbf{s}} = \bar{Z} \circ Z$. If χ is to be a consistent family of projectors, then we must have

$$(3.2) \quad Z\bar{Z}Z = Z.$$

In fact, this equality suffices.

Lemma 3.20. *Suppose that (3.2) is true. Then $\varphi_{\mathbf{y},\mathbf{z}} \circ \varphi_{\mathbf{x},\mathbf{y}} = \varphi_{\mathbf{x},\mathbf{z}}$ and $\chi_{\mathbf{y},\mathbf{z}} \circ \chi_{\mathbf{x},\mathbf{y}} = \chi_{\mathbf{x},\mathbf{z}}$ for all $\mathbf{x}, \mathbf{y}, \mathbf{z} \in \Gamma$.*

It is easier to think about these equalities when one just describes the path, rather than composing the maps ψ . This is because one can read the path in order, rather than backwards (one of the unfortunate features of function notation). So, we will confuse a path morphism with its path.

Proof. The composition $\varphi_{\mathbf{y},\mathbf{z}} \circ \varphi_{\mathbf{x},\mathbf{y}}$ comes from the path

$$\mathbf{x} \searrow \mathbf{t} \nearrow \mathbf{s} \searrow \mathbf{y} \searrow \mathbf{t} \nearrow \mathbf{s} \searrow \mathbf{z}.$$

In the middle, one has the composition $\mathbf{t} \nearrow \mathbf{s} \searrow \mathbf{t} \nearrow \mathbf{s}$ which is just $\bar{Z}Z\bar{Z}$. Using (3.2) to replace this with \bar{Z} , we obtain $\varphi_{\mathbf{x},\mathbf{z}}$. \square

How would one prove (3.2)? One method would be to prove the following equality between path morphisms for each edge $\mathbf{x} \downarrow \mathbf{y}$.

$$(3.3) \quad \mathbf{s} \searrow \mathbf{t} \nearrow \mathbf{y} \downarrow \mathbf{x} \downarrow \mathbf{y} = \mathbf{s} \searrow \mathbf{t} \nearrow \mathbf{y}.$$

In other words, if we go from source to sink, make our way back up to \mathbf{y} , and then apply a little loop, that loop could be deleted.

Lemma 3.21. *Let V be any particular oriented path between source and sink, and suppose that (3.3) holds for each edge $\mathbf{x} \downarrow \mathbf{y}$ in V . Then $Z\bar{Z}Z = Z$.*

Proof. The path yielding $Z\bar{Z}Z$ can be thought of applying Z , going up V , then coming down V . Let $\mathbf{s} = \mathbf{v}_0 \downarrow \mathbf{v}_1 \downarrow \cdots \downarrow \mathbf{v}_m = \mathbf{t}$ be the path V . Letting $\mathbf{x} = \mathbf{s}$ and $\mathbf{y} = \mathbf{v}_1$, $\mathbf{x} \downarrow \mathbf{y}$ is the first edge in V , so we can use (3.3) to replace $\mathbf{s} \searrow \mathbf{t} \nearrow \mathbf{s} \searrow \mathbf{t}$ with $\mathbf{s} \searrow \mathbf{t} \nearrow \mathbf{v}_1 \searrow \mathbf{t}$. Now letting $\mathbf{x} = \mathbf{v}_1$ and $\mathbf{y} = \mathbf{v}_2$, eliminate the second edge of V , replacing $\mathbf{s} \searrow \mathbf{t} \nearrow \mathbf{v}_1 \searrow \mathbf{t}$ with $\mathbf{s} \searrow \mathbf{t} \nearrow \mathbf{v}_2 \searrow \mathbf{t}$. Repeating this argument, we will eventually obtain $\mathbf{s} \searrow \mathbf{t}$, which is Z . \square

Similarly, we can use (3.3) to show that $\chi = \varphi$.

Lemma 3.22. *Let V be any particular oriented path between source and sink, and suppose that (3.3) holds for each edge in V . Then $\varphi_{\mathbf{x},\mathbf{y}} = \chi_{\mathbf{x},\mathbf{y}}$ for any two vertices along the path V .*

Proof. By the same argument used in the proof of Lemma 3.21, we know that for any \mathbf{x} in V one has an equality of path morphisms

$$(3.4) \quad \mathbf{s} \searrow \mathbf{t} \nearrow \mathbf{s} \searrow \mathbf{x} = \mathbf{s} \searrow \mathbf{t} \nearrow \mathbf{x}.$$

Thus

$$\begin{aligned} \varphi_{\mathbf{x}, \mathbf{y}} &= \mathbf{x} \searrow \mathbf{t} \nearrow \mathbf{s} \searrow \mathbf{y} = \mathbf{x} \searrow \mathbf{t} \nearrow \mathbf{s} \searrow \mathbf{t} \nearrow \mathbf{s} \searrow \mathbf{y} = \\ &= \mathbf{x} \nearrow \mathbf{s} \searrow \mathbf{t} \nearrow \mathbf{s} \searrow \mathbf{y} = \mathbf{x} \nearrow \mathbf{s} \searrow \mathbf{t} \nearrow \mathbf{y}. \end{aligned}$$

First we replaced \overline{Z} with $\overline{ZZ}\overline{Z}$, then applied the upside-down version of (3.4) to \mathbf{x} , and then applied (3.4) to \mathbf{y} . \square

The bulk of the computations in this chapter go into proving (3.3) for just one path V , a path that we choose very carefully for its nice combinatorial properties! It would be nice to have a more path-independent proof of these results.

Let us quickly discuss how this works. The equality (3.3) really wants to replace the doubled 6-valent vertex $\mathbf{y} \uparrow \mathbf{x} \downarrow \mathbf{y}$ with the identity map of \mathbf{y} . But these are two different morphisms, and the difference between them is the other idempotent in (2.27), which factors through the aborted 6-valent vertex (2.34). Thus (3.3) is implied by

$$(3.5) \quad A_{\mathbf{y} \uparrow \mathbf{x}} \psi_{\mathbf{t} \nearrow \mathbf{y}} Z = 0.$$

where $A_{\mathbf{y} \uparrow \mathbf{x}}$ is the aborted 6-valent vertex, instead of the 6-valent vertex, an *aborted edge*. We think of the composition $A_{\mathbf{y} \uparrow \mathbf{x}} \psi_{\mathbf{t} \nearrow \mathbf{y}}$ as being an aborted version of \overline{V} . So, said quickly, (3.5) is the statement that Z is orthogonal to aborted versions of \overline{Z} .

This is what we prove, painstakingly, throughout the next several sections, for a special path V . Using a combinatorial description of V , we describe every possible abortion of V , and check this orthogonality property. The path V that we use is inductively defined and behaves reasonably well for the inclusion of the longest element of S_n inside the longest element of S_{n+1} . We isolate how the aborted 6-valent vertex behaves with respect to the ‘‘inductive’’ part of the part V , which will be the path FR_1 defined in Definition 3.31.

So, having proven (3.3), we know that φ is a consistent family of projectors. We prove in §3.6 that the image of φ_J (coming from the graph Γ_{w_J}) is the indecomposable B_J corresponding to w_J . The proof follows the lines of Proposition 2.16. Let X temporarily denote the image of φ . We construct a morphism a_i in §3.4, one for each $i \in J$, and compute that it descends to a map from $X \otimes i$ to X of degree -1 . Using a_i , we construct the inclusions and projections in a decomposition $X \otimes i \cong X(1) \oplus X(-1)$. Then, using orthogonality results like (3.5), we prove that the Hom space $\text{HOM}(X, \emptyset)$ is at most rank 1, generated by a specific morphism ξ_J in degree d_J . We check that ξ_J is nonzero by applying the functor to bimodules. Put together, these facts and Proposition 2.16 imply that $X \cong B_J$.

We also prove a number of properties of the maps a_i , which will simplify the thick calculus. We introduce a_i before proving that φ is a consistent family of projectors because it will be useful in the inductive proof of (3.5).

Once we know that the image of φ_J in the Grothendieck group is b_J , we can then prove that everything which was true for our specific path V also holds for a general path.

Lemma 3.23. *The family φ_J is orthogonal to any aborted 6-valent vertex.*

Proof. The following is a simple exercise in the Hecke algebra which requires some knowledge of the standard basis and the Deodhar formula. For an arbitrary sequence \underline{i} of length k , rewriting $b_{i_1} b_{i_2} \cdots b_{i_k}$ in the standard basis $\{H_w\}$, the coefficient of H_w is zero when $\ell(w) > k$, and otherwise has minimal degree greater than or equal to $-(k - \ell(w))$. In particular, in the

standard pairing, $(b_w, b_{i_1} b_{i_2} \cdots b_{i_k})$ has no degree 0 component if $\ell(w) > k$ and b_w is smooth (all the Kazhdan-Lusztig polynomials are 1).

Now let \underline{i} be the target of an aborted 6-valent vertex. That is, \underline{i} has length $d_J - 2$, and is a reduced expression for w_J with some $s_i s_j s_i$ replaced by s_i , for $i, j \in J$ adjacent. Then there are no degree 0 maps from B_J to \underline{i} , and the aborted 6-valent vertex must be orthogonal to the projection to B_J . \square

Proposition 3.24. *The equality (3.3) holds for all edges. In addition, for any edge from \mathbf{x} to \mathbf{y} in $\tilde{\Gamma}$, the composition of $\varphi_{\mathbf{z}, \mathbf{x}}$ with this edge is $\varphi_{\mathbf{z}, \mathbf{y}}$.*

Proof. Using (2.27), the difference between $\mathbf{y} \uparrow \mathbf{x} \downarrow \mathbf{y}$ and the identity of \mathbf{y} factors through an aborted 6-valent vertex, and is orthogonal to φ_J . This proves (3.3). Now consider an edge from \mathbf{x} to \mathbf{y} in $\tilde{\Gamma}$. If it is a distant edge or an oriented edge, adding this edge to the path for $\varphi_{\mathbf{z}, \mathbf{x}}$ yields precisely the path for $\varphi_{\mathbf{z}, \mathbf{y}}$. If it is a reverse oriented edge, we use (3.3) (or its flipped version) to deduce the desired equality. \square

In particular, this implies that $\chi = \varphi$ everywhere using Lemma 3.22.

Now we begin the long and nasty proof of (3.5) with a study of various vertices and paths between them in $\tilde{\Gamma}$.

3.3. The longest element. We fix notation for several useful vertices in $\tilde{\Gamma}$ lying over \mathbf{s} and \mathbf{t} . We will use a subscript J when describing the corresponding construction in $\tilde{\Gamma}_{w_J}$ for a connected parabolic subset J .

Notation 3.25. (Example: $n = 5$) We write \mathbf{s}^R for the lexicographically minimal expression, which was given at the beginning of §3.2, e.g. 1 21 321 4321 54321. Note that $\mathbf{s}^R = \mathbf{s}_K^R$ 54321 for $K = \{1, 2, 3, 4\}$. We write \mathbf{s}^L for the horizontal flip of the default sequence, also thought of as the “left-facing” default sequence, $\mathbf{s}^L = 12345$ 1234 123 12 1 = $12345\mathbf{s}_K^L$.

Remark 3.26. Here and elsewhere, we will be illustrating various proofs and definitions by using examples. This is a dangerous practice, but we solemnly promise that the general case truly will be evident to the reader after a brief study of the examples (or so we hope!). We will be drawing path morphisms soon enough, and it is incredibly inconvenient to draw a general case; while the general case could be made explicit symbolically, the advantage of graphical calculus is lost when one passes to long strings of symbols. The examples we give will be more enlightening.

Notation 3.27. Now we look for expressions interpolating between \mathbf{s}^R and \mathbf{s}^L . Let $i \in I$, and let $M_i = \{1, 2, \dots, i\}$. Then we write \mathbf{s}_i^R for the sequence that begins as \mathbf{s}^L until $i + 1$, i.e. with 12345 1234 ... 12 ... $(i + 1)$ and then concludes with $\mathbf{s}_{M_i}^R$. Note that $\mathbf{s}_n^R = \mathbf{s}^R$. Explicitly,

- $\mathbf{s}_5^R = \mathbf{s}^R = 1\ 21\ 321\ 4321\ 54321$,
- $\mathbf{s}_4^R = 12345\ 1\ 21\ 321\ 4321$,
- $\mathbf{s}_3^R = 12345\ 1234\ 1\ 21\ 321$,
- $\mathbf{s}_2^R = 12345\ 1234\ 123\ 1\ 21 = 12345\ 1234\ 123\ 12\ 1 = \mathbf{s}_1^R = \mathbf{s}^L$.

Flipping all of these horizontally, we get $\mathbf{s}_i^L = \mathbf{s}_{I, i}^L$.

We have put spacing in our reduced expressions just to make it easier for the reader to parse, but the spaces have no mathematical significance.

To get from \mathbf{s}_5^R to \mathbf{s}_4^R , simply find the first instance of each index 12345 (which is the start of each segment separated by the spaces), and commute them to the left as far as possible, until the sequence begins with 12345. That this is possible can be proven inductively. Note

that $\mathbf{s}_4^R = 12345\mathbf{s}_K^R = 12345\mathbf{s}_{K,4}^R$ for $K = \{1, 2, 3, 4\}$. The transformation from \mathbf{s}_4^R to \mathbf{s}_3^R does not affect the initial sequence 12345, and is just the inductively defined operation from $\mathbf{s}_{K,4}^R$ to $\mathbf{s}_{K,3}^R$ on the remainder. Thus one can travel from any \mathbf{s}_i^R to any \mathbf{s}_j^R using only distant edges in $\tilde{\Gamma}$, which justifies that they all lie over \mathbf{s} .

The salient feature of \mathbf{s}_i^R is that, reading from the right, it begins with an expression for the longest element of $M_i = \{1, 2, \dots, i\}$. We will see that when $B_{\mathbf{s}}$ interacts with other colors on the right, and those other colors are in M_i , then \mathbf{s}_i^R is the most useful representative of the isomorphism class, because the parts on the left (123451234 when $i = 3$) will not play an important role. This will become clear in examples to come.

Notation 3.28. Similarly, let $\mathbf{t}^R = 5\ 45\ 345\ 2345\ 12345 = \mathbf{t}_1^R$ be the lexicographically maximal expression, also given at the beginning of §3.2. Let $\mathbf{t}_2^R = 54321\ 5\ 45\ 345\ 2345$, and so forth, with \mathbf{t}_i^L being the horizontal flips. Here, we think of M_i as being $\{i, i+1, \dots, n\}$.

Now we introduce several paths in $\tilde{\Gamma}$. For the rest of the paper, we use the colors blue, red, green, purple, and black to represent the indices 1, 2, 3, 4, 5 respectively.

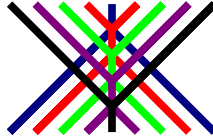


Definition 3.29. First, we introduce a useful path on subexpressions. For $i < j$ let $F = F_{i,j}$ denote the *flip* path, defined by example here:

$$F_{1,4} = 1234321 \mid 1243421 = 4123214 \mid 4132314 = 4312134 \mid 4321234,$$

$$F_{3,5} = 34543 \mid 35453 = 53435 \mid 54345.$$

In general, $F_{i,j}$ starts at the sequence going from i up to j and back down to i , and repeatedly applies an adjacent edge to the middle until the final expression is reached. We will usually just call the flip map F when the indices are understood, and also use the same notation F for the opposite path to this one. The flip path F can also be viewed as the unique oriented path from source to sink in Γ_v for v the appropriate permutation. Here is the path morphism for $F_{1,5}$.



This diagram is exactly the path described above, up to “monoidal operations,” that is, up to disjoint squares in $\tilde{\Gamma}$.

Definition 3.30. Next, we inductively define a specific path $V = V^R$ from $\mathbf{s}^R \searrow \mathbf{t}^R$. When $n = 1$, $\mathbf{s} = \mathbf{t}$ and the path is trivial. Suppose we have defined V_J for all connected J .

(Example: $n = 5$) Let us define V by example. Let $K = \{1, 2, 3, 4\}$. Then $\mathbf{s}^R = s_K^R 54321$. To obtain V , first we apply V_K to get $t_K^R 54321 = 4\ 34\ 234\ 1234\ 54321$, and then we apply a sequence of flip maps of decreasing size $4\ 34\ 234\ \underline{123454321} \searrow 4\ 34\ \underline{2345432} \ 12345 \searrow 4\ \underline{34543} \ 2345\ 12345 \searrow \underline{454} \ 345\ 2345\ 12345 \searrow 5\ 45\ 345\ 2345\ 12345 = \mathbf{t}^R$.

(Example: $n = 4$) Here is the picture of V :

(3.6)

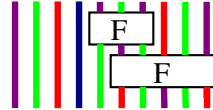
The path V will be one of our preferred paths from \mathbf{s} to \mathbf{t} , and thus a preferred realization of the morphism Z . Before proving facts about Z , we will need to describe several other important paths.

Definition 3.31. (Example: $n = 4$) We introduce some paths in Γ which use compositions of flip maps to bring certain indices to the far right. We think of them as paths in Γ because we will be flexible as to which equivalence class of reduced expression we use for the source and sink.

Note that the expression $\mathbf{t}^R = 4\ 34\ 234\ 1234$ has a single instance of the index 1. To bring 1 to the far right, we can apply the following sequence of (reverse) flip maps: $4\ 34\ 234\ 1234 \nearrow 3\ 43\ 234\ 1234 \nearrow 3\ 23\ 432\ 1234 \nearrow 3\ 23\ 123\ 4321$. We denote this sequence of flips by $\overline{FR}_{\mathbf{t},1}$, and let us denote the sequence in reverse by $FR_{\mathbf{t},1}$. In (3.6) above, the path V ends in a sequence of flips, which is exactly $FR_{\mathbf{t},1}$.

The notation in $\overline{FR}_{\mathbf{t},1}$ is chosen because it takes index 1 from \mathbf{t} and Flips it to the Far Right. We let $FR_{\mathbf{t},1}$ have no overline because it is an oriented map, while $\overline{FR}_{\mathbf{t},1}$ is reverse-oriented. We will not introduce notation for the source of $FR_{\mathbf{t},1}$, which is some vertex in Γ .

Now let us define $\overline{FR}_{\mathbf{t},2}$, which brings the index 2 to the far right with a minimal sequence of flips. We begin with $\mathbf{t}_2^R = 4321\ 434234$, and then apply the flip maps $4321\ 434234 \nearrow 4321\ 343234 \nearrow 4321\ 323432$. Similarly, we define $FR_{\mathbf{t},2}$ to be the reverse map, which is pictured below.



To define $\overline{FR}_{\mathbf{t},i}$, which brings the index i to the far right, we begin with \mathbf{t}_i^R , which by definition ends in $\mathbf{t}_{M_i}^R$ where $M_i = \{i, \dots, n\}$. Then, to the subsequence $\mathbf{t}_{M_i}^R$, we apply the flip sequence $\overline{FR}_{\mathbf{t}_{M_i},i}$ which has been inductively defined. Thus our final two examples for $n = 4$ are $\overline{FR}_{\mathbf{t},3}: 4321432\ 434 \nearrow 4321432\ 343$, and the identity map $\overline{FR}_{\mathbf{t},4}: 432143243\ 4 \rightarrow 432143243\ 4$. The sources of the map $\overline{FR}_{\mathbf{t},i}$ are various different expressions in $\tilde{\Gamma}$ which lift \mathbf{t} , but since we view $\overline{FR}_{\mathbf{t},i}$ as a path in Γ , the all have the same source \mathbf{t} .

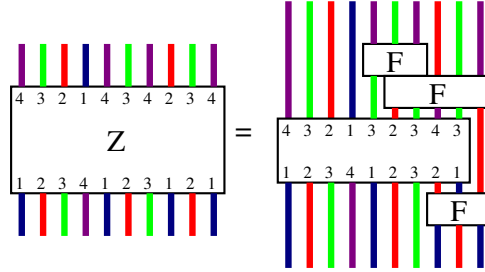
In similar fashion, we can define $FR_{\mathbf{s},i}$, which brings the index i to the far right, starting from \mathbf{s} . Now it is $FR_{\mathbf{s},4}$ which is the most complicated, and $FR_{\mathbf{s},1}$ which is the identity map. For example, $FR_{\mathbf{s},4}$ begins with $\mathbf{s}^R = 1213214321$ and applies the flips $1213214321 \searrow 2123214321 \searrow 2321234321 \searrow 2324321234$. Similarly, $FR_{\mathbf{s},3}$ begins with $\mathbf{s}_3^R = 1234\ 121321$ and applies the flips $1234\ 121321 \searrow 1234\ 212321 \searrow 1234\ 232123$. As before, we define $\overline{FR}_{\mathbf{s},i}$ to be the reverse path, and note that the version without the overline is an oriented path.

Finally, we can also define $FL_{\mathbf{t},i}$ and $FL_{\mathbf{s},i}$, which Flip the index i to the Far Left. These are the horizontal reflections of the above.

Claim 3.32. Fix any $i \in I$. Let $FR_{\mathbf{s},i}: \mathbf{s} \searrow \mathbf{x}$ and $FR_{\mathbf{t},i}: \mathbf{y} \searrow \mathbf{t}$ be the oriented paths defined above, so that x and y are both expressions with i on the far right. Then there is an oriented path $x \searrow y$ which does not alter the rightmost index i .

This claim allows one to factor the path morphism $Z: \mathbf{s} \searrow \mathbf{t}$ as $\mathbf{s} \searrow \mathbf{x} \searrow \mathbf{y} \searrow \mathbf{t}$. This is another useful path denoted V_i , which is adapted to the index i . Note that $V = V_1$.

Example 3.33. (Example: $n = 4$) When $i = 2$, we have



where the unlabeled box represents some unspecified oriented path. We have chosen the source and target of this morphism to be \mathbf{s}_2^R and \mathbf{t}_2^R respectively. The flip below the mystery box is $FR_{\mathbf{s},2}$ and the flip sequence above the box is $FR_{\mathbf{t},2}$.

Proof. Let $\hat{\mathbf{x}}$ denote the expression \mathbf{x} without the final index i . Technically, this is an equivalence class of expressions for w_0s_i , living in $\Gamma_{w_0s_i}$. Define $\hat{\mathbf{y}} \in \Gamma_{w_0s_i}$ similarly. We need to show that there is an oriented path $\hat{\mathbf{x}} \searrow \hat{\mathbf{y}}$ in $\Gamma_{w_0s_i}$.

First, consider the special case where $i = 1$. Then $\mathbf{x} = \mathbf{s}$, and $\hat{\mathbf{x}}$ is the (unique) source of the expression graph for w_0s_1 . Thus there is an oriented path $\hat{\mathbf{x}} \searrow \hat{\mathbf{y}}$. Similarly, when $i = n$, $\hat{\mathbf{y}}$ is the unique sink for w_0s_n .

Now, consider the example when $n = 7$ and $i = 3$. Then

$$\mathbf{x} = 1234567 \ 123456 \ 12345 \ 1234 \ \mathbf{x}', \quad \mathbf{y} = 7654321 \ 765432 \ \mathbf{y}'.$$

Here, \mathbf{x}' is the target of the flip map FR_3 from $\mathbf{s}_{\{1,2,3\}}$, and \mathbf{y}' is the source of the flip map FR_3 to $\mathbf{t}_{\{3,4,5,6,7\}}$. We know by the special cases above that there are oriented maps $\mathbf{x}' \searrow \mathbf{t}_{\{1,2,3\}}$ and $\mathbf{s}_{\{3,4,5,6,7\}} \searrow \mathbf{y}'$ which do not involve the final index 3. So, replacing \mathbf{x}' with $\mathbf{t}_{\{1,2,3\}}$ and \mathbf{y}' with $\mathbf{s}_{\{3,4,5,6,7\}}$, it is enough to show that there is an oriented path of the form

$$(3.7) \quad 1234567 \ 123456 \ 12345 \ 1234 \ (321 \ 32 \ 3) \ \searrow \quad 7654321 \ 765432 \ (34567 \ 3456 \ 345 \ 34 \ 3)$$

which does not involve the final index 3.

Let us apply a sequence of flip maps:

$$1234567 \ 123456 \ 12345 \ \underline{1234 \ 321} \ 32 \ 3 \ \searrow \ 1234567 \ 123456 \ \underline{12345 \ 4321} \ 234 \ 32 \ 3 \ \searrow \dots \\ \searrow \ 7654321 \ 234567 \ 23456 \ 2345 \ 234 \ (32 \ 3).$$

The result begins with 7654321 as does our desired target. Removing 7654321 from both source and target, the remainder is actually of exactly the form (3.7), except for the parabolic subset $\{2, 3, 4, 5, 6, 7\}$ instead of $\{1, 2, 3, 4, 5, 6, 7\}$. Now, induction finishes the proof. \square

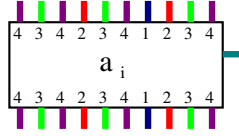
3.4. Thick trivalent vertices. When we have fixed a parabolic subset $J \subset I$ and wish to express an arbitrary index $i \in J$, we use either the color teal or brown.



Because $B_J \otimes B_i \cong B_J(1) \oplus B_J(-1)$ for $i \in J$, there should be some projection/inclusion maps between $B_J \otimes B_i$ and B_J of degree ± 1 . When $J = \{i\}$ so that $B_J = B_i$, we know that the projection map of degree -1 is drawn as a trivalent vertex (as is the inclusion map of degree -1 , since they are related under biadjunction). Whatever they are for B_J , we should think of the projection (resp. inclusion) map of degree -1 as a *thick trivalent vertex*.

Once we prove that φ_J is a consistent family of projectors, Remark 2.15 states that we can specify a map $B_J \otimes B_i \rightarrow B_J$ by giving a map from $B_{\mathbf{x}} \otimes B_i \rightarrow B_{\mathbf{x}}$, for some reduced expression \mathbf{x} for w_J , which is preserved under pre-composition with $\varphi_{\mathbf{x},\mathbf{x}} \otimes 1_i$ and post-composition with $\varphi_{\mathbf{x},\mathbf{x}}$. Alternatively, we can provide any map $B_{\mathbf{x}} \otimes B_i \rightarrow B_{\mathbf{x}}$, and then pre- and post-compose it as above. The map we provide will be named $a_{\mathbf{x},i}^R$, where the R indicates that the new i -colored strand is on the Right. Pre-composing a with $\varphi_{\mathbf{x},\mathbf{x}} \otimes 1_i$ and post-composing with $\varphi_{\mathbf{x},\mathbf{x}}$, we obtain the map which descends to the thick trivalent vertex.

For example, the map $a_{\mathbf{t}_J,i}^R$ has the following form, when $J = \{1, 2, 3, 4\}$.

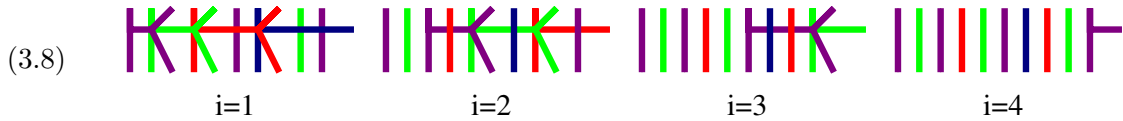


Teal represents the arbitrary index $i \in J$. We have rotated the picture so that i appears as a side boundary instead of a bottom boundary.

Similarly, since $B_i \otimes B_J$ also splits into two copies of B_J , there should be a thick trivalent vertex on the left as well. The horizontal flip of $a_{\mathbf{t}_J,i}^R$ above would be $a_{\mathbf{t}_J,i}^L$, which creates an i -labeled strand on the left, and uses the expression \mathbf{t}_J^L . For these maps, \mathbf{x} and i can be determined from the colors on the boundary, and R or L determined by where the additional teal line sticks out, so we will often call it simply a_i or a . When the parabolic subset J is not written, it is assumed to be the entire set I .

We have not yet proven that φ_J is a consistent family of projectors, but we will at least define $a_{\mathbf{x},i}^R$ for all reduced expressions \mathbf{x} lifting \mathbf{s} and \mathbf{t} , and check that it commutes appropriately with $\varphi_{\mathbf{s},\mathbf{s}}$ and $\varphi_{\mathbf{s},\mathbf{t}}$. In fact, the basic principle is this: when \mathbf{x} has i on the right, the thick trivalent vertex comes from an ordinary trivalent vertex (composed with φ). When it does not, they are intertwined by the path morphism which brings i to the right, namely FR_i . This is confirmed in (3.12) and (3.16) below.

Definition 3.34. (Example: $n = 4$) Let the morphism $a_{\mathbf{t}_R,i}^R$ be the morphism described in the following examples. It has top and bottom boundary \mathbf{t}^R and side boundary i .



Read this morphism from right to left. When $i = n$, the result is just a trivalent vertex. Otherwise, the i -strand comes from the right, crosses left over any strands with labels $\geq i + 2$, and then meets the strand labeled $i + 1$ in a 6-valent vertex. Then, the strand labeled $i + 1$ crosses left over any strands with labels $\leq i - 1$. What remains on bottom and top is the reduced expression $\mathbf{t}_{\{2,3,\dots,n\}}^R$, with $i + 1$ coming in from the right. Then, the process is repeated inductively for the $i + 1$ strand.

Any expression \mathbf{x} for w_0 which lives above \mathbf{t} is connected to any other by a sequence of distant edges, and these distant edges form a compatible family of isomorphisms, as previously

discussed. Thus we may define $a_{\mathbf{x},i}^R$ to be the morphism intertwined with $a_{\mathbf{t}^R,i}^R$ by these isomorphisms. We let $a_{\mathbf{t},i}^R$ denote this family. To give an example, here is the morphism $a_{\mathbf{t}_i^R,i}^R$, which has top and bottom boundary \mathbf{t}_i^R instead.

$$(3.9) \quad \begin{array}{cccc} \text{Diagram 1} & \text{Diagram 2} & \text{Diagram 3} & \text{Diagram 4} \\ \text{i=1} & \text{i=2} & \text{i=3} & \text{i=4} \end{array}$$

This version of a_i is possibly more intuitive, as it has fewer needless 4-valent vertices. When $i = 1$, $\mathbf{t}_1^R = \mathbf{t}^R$ and the diagram is as complicated as before. Otherwise, it decomposes as identity maps next to $a_{\mathbf{t}_{J,i}^R,i}^R$ for $J = M_i = \{i, \dots, n\}$.

Similarly, one can define $a_i = a_{\mathbf{s}^R,i}^R$ as follows.

$$(3.10) \quad \begin{array}{cccc} \text{Diagram 1} & \text{Diagram 2} & \text{Diagram 3} & \text{Diagram 4} \\ \text{i=4} & \text{i=3} & \text{i=2} & \text{i=1} \end{array}$$

One can use this to define $a_{\mathbf{x},i}^R$ for any expression lifting \mathbf{s} .

Now it is time to gather some results about the various maps a_i, FR_i, Z , in an effort to prove that a_i interacts nicely with $\varphi_{\mathbf{s},\mathbf{t}}$ and $\varphi_{\mathbf{s},\mathbf{s}}$. The key relation, which leads to all the others, is the following:

Claim 3.35. (Example: $n = 5$) We have the following equality.

$$(3.11) \quad \begin{array}{c} \text{Diagram 1} \\ \text{Diagram 2} \end{array} = \begin{array}{c} \text{Diagram 3} \\ \text{Diagram 4} \end{array} \cdot$$

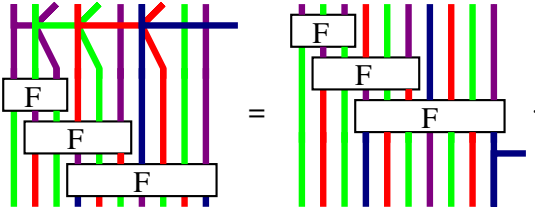
Proof. Writing out the flip map in full, this is an immediate application of relation (2.30). Explicitly,

$$\begin{array}{c} \text{Diagram 1} \\ \text{Diagram 2} \\ \text{Diagram 3} \\ \text{Diagram 4} \end{array} = \begin{array}{c} \text{Diagram 5} \\ \text{Diagram 6} \\ \text{Diagram 7} \\ \text{Diagram 8} \end{array}$$

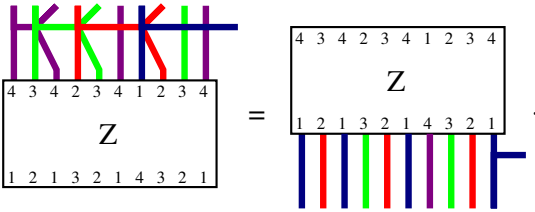
The box labelled F in the intermediate calculations is the flip map for $\{2, 3, 4, 5\}$. □

We now demonstrate some of this nice behavior for a_1 .

Claim 3.36. We have the following equalities, dealing with a_1 . The first two are examples for $n = 4$.

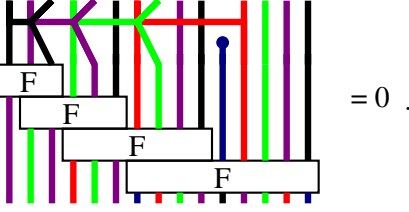
(3.12) 

Symbolically, this is $a_1 = a_{tR,i}^R$ put above $FR_{t,1}$.

(3.13) 

Once again, the diagram above Z on the LHS is a_1 . The trivalent vertex below Z on the RHS also happens to be $a_1 = a_{sR,1}^R$.

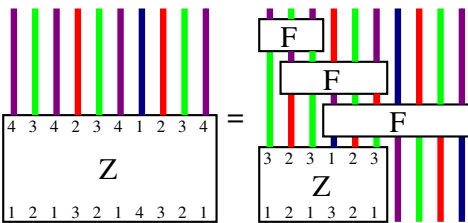
This last equation is not motivated at the moment, but will be used to deal with “abortion terms” in a future calculation. This is the $n = 5$ example.

(3.14) 

The upper left corner looks like (3.12) but for $J = \{2, 3, 4, 5\}$. The bottom is the flip sequence $FR_{t,1}$ for $\{1, 2, 3, 4, 5\}$.

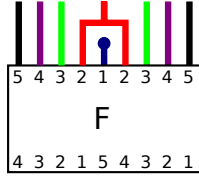
Proof. The equality (3.12) is easily seen to be an iterated use of (3.11), starting with the leftmost flip and moving to the right.

To get (3.13), remember that we can always express Z as

(3.15) 

using the path V , see (3.6). Placing $Z_{\{1,2,3\}}$ below (3.12) yields (3.13).

Applying (3.12) to all but the last flip in (3.14), the diagram factors through the following picture as it enters the final flip:



This factoring was observed in (2.36). However, the first thing that happens in a flip is a 6-valent vertex, which kills the aborted 6-valent vertex by (2.35) \square

It may be useful for the reader to work through the examples of $n = 2, 3$ explicitly, writing out flip maps and Z in full and checking these results. The general computations are no more difficult.

The claim above could be thought of as a suite of results about a_1 . Now we generalize these results to a_i for any i .

Claim 3.37. *We have the following equalities, for any $i \in I$. Each expression has an arbitrary expression lifting \mathfrak{t} as the target. The map a_i represents either $a_{\mathfrak{t},i}^R$ or $a_{\mathfrak{s},i}^R$. The map FR_i is $FR_{\mathfrak{t},i}$. As usual, \bar{Z} represents Z upside-down.*

$$(3.16) \quad \begin{array}{|c|} \hline a_i \\ \hline FR_i \\ \hline \end{array} = \begin{array}{|c|} \hline FR_i \\ \hline \end{array} .$$

$$(3.17) \quad \begin{array}{|c|} \hline a_i \\ \hline \begin{array}{c} 4\ 3\ 4\ 2\ 3\ 4\ 1\ 2\ 3\ 4 \\ Z \\ 1\ 2\ 1\ 3\ 2\ 1\ 4\ 3\ 2\ 1 \end{array} \\ \hline \end{array} = \begin{array}{|c|} \hline \begin{array}{c} 4\ 3\ 4\ 2\ 3\ 4\ 1\ 2\ 3\ 4 \\ Z \\ 1\ 2\ 1\ 3\ 2\ 1\ 4\ 3\ 2\ 1 \end{array} \\ \hline a_i \\ \hline \end{array} .$$

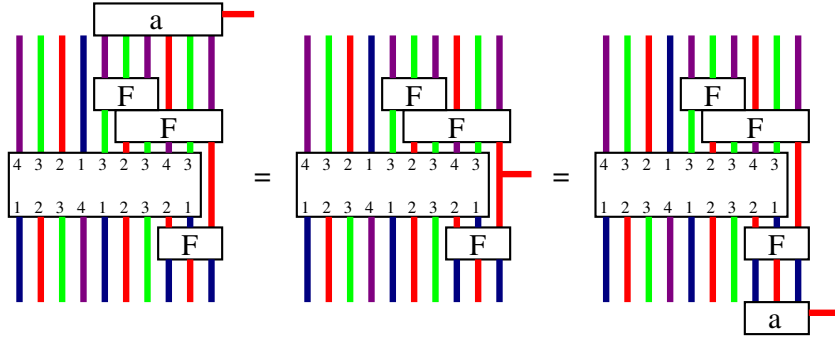
$$(3.18) \quad \begin{array}{|c|} \hline a_i \\ \hline Z \\ \hline \bar{Z} \\ \hline \end{array} = \begin{array}{|c|} \hline Z \\ \hline \bar{Z} \\ \hline a_i \\ \hline \end{array} .$$

$$(3.19) \quad \begin{array}{|c|} \hline a_i \\ \hline a_i \\ \hline Z \\ \hline \end{array} = \begin{array}{|c|} \hline a_i \\ \hline Z \\ \hline \end{array} .$$

In particular, (3.17) says that our maps $a_{\mathfrak{t},i}$ and $a_{\mathfrak{s},i}$ are intertwined by Z , and (3.18) says that $a_{\mathfrak{t},i}$ commutes with $\varphi_{\mathfrak{t},\mathfrak{t}}$.

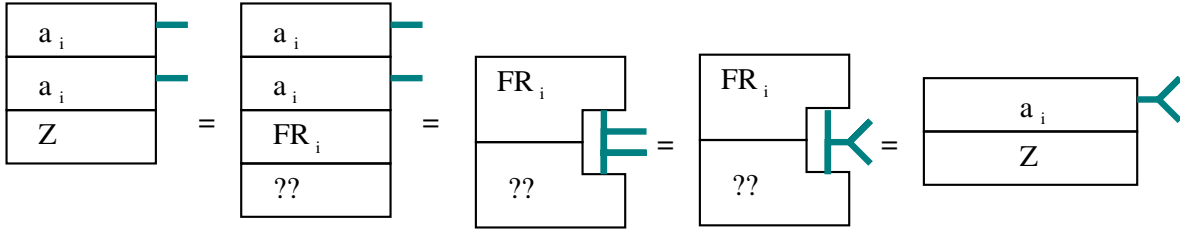
Proof. To prove (3.16), let us choose \mathfrak{t}_i^R to be our target, and use the description of a_i given in (3.9). If $i = 1$ then (3.16) is (3.12). Otherwise, both a_i and FR_i are expressed as a tensor product of an identity morphism, and the corresponding maps for the parabolic subset $M_i = \{i, \dots, n\}$. This reduces the equality to (3.12) for M_i .

To prove (3.17), we simply use the path V_i of Claim 3.32 and apply (3.16) twice. We provide an example, for $n = 4$ and $i = 2$. The target is chosen to be t_i^R , and the source to be s_i^R . The flip sequences above the mystery box is $FR_{t,i}$, and the flip sequence below it is $FR_{s,i}$.



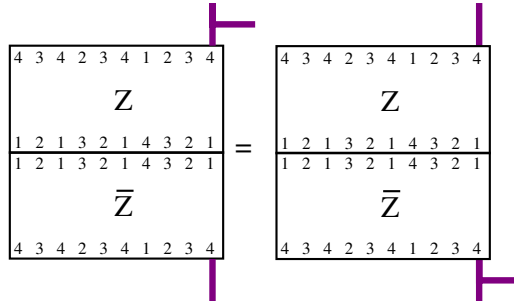
Applying (3.17) twice, we immediately get (3.18).

To obtain (3.19), we again use the path V_i , and proceed as follows.



□

Corollary 3.38. (Example: $n = 4$). We have the following equality.



Proof. This is a special case of (3.18), when $i = n$. □

We now show that Z is orthogonal to certain aborted versions of a_i . This is the first step towards a proof of (3.5), and will also be used to describe some additional properties of a_i below.

Proposition 3.39. (Example: $n = 5$) The maps of Figure 1 are all zero.

Remark 3.40. To the reader familiar with light leaves from [EW] or [Lib08], this proposition (with the factorization discussed near (2.36)) states that Z is orthogonal to certain light leaves of degree zero. It is possible that many statements in this chapter can be streamlined by introducing light leaves, though it is not clear that the proofs would be.

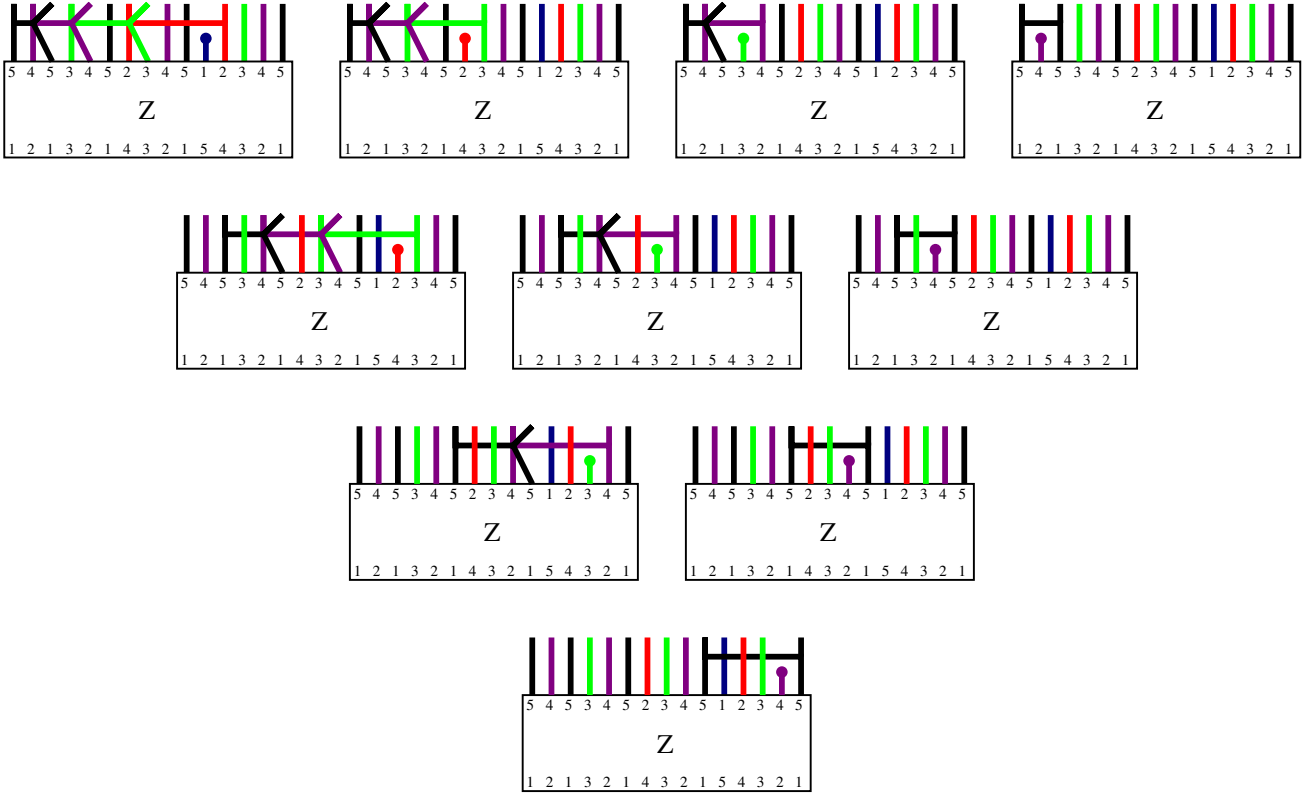


FIGURE 1. The morphisms in Proposition 3.39

Proof. This is a generalization of (3.14), and follows quickly from it. The first picture of the first row is precisely that of (3.14), while the second picture is what (3.14) would be for $K = \{2, 3, 4, 5\}$ with additional lines 12345 added on the right. Choosing a path $\mathbf{s} \searrow \mathbf{t}$ which ends by applying V_K on the left, the map is zero by the K case of (3.14). The third picture in the first row is zero by the $K = \{3, 4, 5\}$ case, and so forth.

For the second row, as for a_2 , we slide 54321 to the left and ignore it (that is, we were better off using \mathbf{t}_2^R instead of \mathbf{t}^R). Then, letting $K = \{2, 3, 4, 5\}$, we are left with what would be the first row for (3.39) for K . We leave a more explicit version to the reader. Similarly, for the third row, we slide 543215432 to the left, and what remains is the first row for $K = \{3, 4, 5\}$. The pattern is now clear. \square

We conclude this section with some further properties of a_i , which will simplify our thick calculus in §4. The first one states that (3.19) holds true, even without Z below. The proof of (3.19) used the existence of Z and the path V_i to simplify the proof drastically, while the proof below is an annoying computation. The same statement is true for the other statements here: they are easier to prove when Z is placed below them, and we leave these easier proofs as exercises for the reader. In fact, we will only ever care about the maps a_i when they are being post- or pre-composed with Z or \bar{Z} . Nonetheless, the properties below mostly hold in the absence of Z , so they might as well be proven there.

Proposition 3.41. *The following equations hold, as endomorphisms of (some lift of) \mathbf{s}_J .*

For any $i \in J$:

$$(3.20) \quad \begin{array}{|c|} \hline a_i \\ \hline a_i \\ \hline \end{array} \begin{array}{l} \text{---} \\ \text{---} \end{array} = \begin{array}{|c|} \hline a_i \\ \hline \end{array} \begin{array}{l} \text{---} \\ \text{---} \end{array}$$

When teal is $i \in J$ and brown is $i + 1 \in J$:

$$(3.21) \quad \begin{array}{|c|} \hline a_i \\ \hline a_j \\ \hline a_i \\ \hline \end{array} \begin{array}{l} \text{---} \\ \text{---} \\ \text{---} \end{array} = \begin{array}{|c|} \hline a_j \\ \hline a_i \\ \hline a_j \\ \hline \end{array} \begin{array}{l} \text{---} \\ \text{---} \\ \text{---} \end{array}$$

When teal is $i \in J$ and brown is $i + 1 \in J$ (this does require Z below):

$$(3.22) \quad \begin{array}{|c|} \hline a_i \\ \hline a_j \\ \hline a_i \\ \hline \bar{Z} \\ \hline \end{array} \begin{array}{l} \text{---} \\ \text{---} \\ \text{---} \end{array} = \begin{array}{|c|} \hline a_j \\ \hline a_i \\ \hline a_j \\ \hline \bar{Z} \\ \hline \end{array} \begin{array}{l} \text{---} \\ \text{---} \\ \text{---} \end{array}$$

For any $i, j \in J$ distant:

$$(3.23) \quad \begin{array}{|c|} \hline a_i \\ \hline a_j \\ \hline \end{array} \begin{array}{l} \text{---} \\ \text{---} \end{array} = \begin{array}{|c|} \hline a_j \\ \hline a_i \\ \hline \end{array} \begin{array}{l} \text{---} \\ \text{---} \end{array}$$

For any $i, j \in J$, with no restrictions ($i = j$ is possible):

$$(3.24) \quad \begin{array}{|c|} \hline a_i \\ \hline a_j \\ \hline \end{array} \begin{array}{l} \text{---} \\ \text{---} \end{array} = \begin{array}{|c|} \hline a_j \\ \hline a_i \\ \hline \end{array} \begin{array}{l} \text{---} \\ \text{---} \end{array}$$

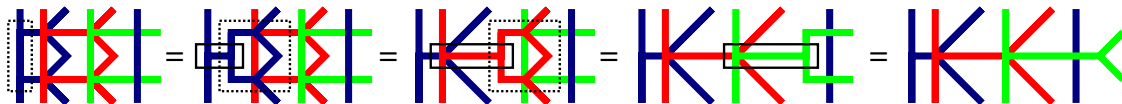
For any $i \in J$ (this does require Z below):

$$(3.25) \quad \begin{array}{|c|} \hline a_i \\ \hline \bar{Z} \\ \hline \end{array} \begin{array}{l} \text{---} \\ \text{---} \end{array} = \begin{array}{|c|} \hline \bar{Z} \\ \hline \end{array} \begin{array}{l} \text{---} \\ \text{---} \end{array}$$

These equations (modifying Z and \bar{Z} appropriately) also hold as endomorphisms of (some lift of) \mathfrak{t}_J . One should swap (3.21) and (3.22).

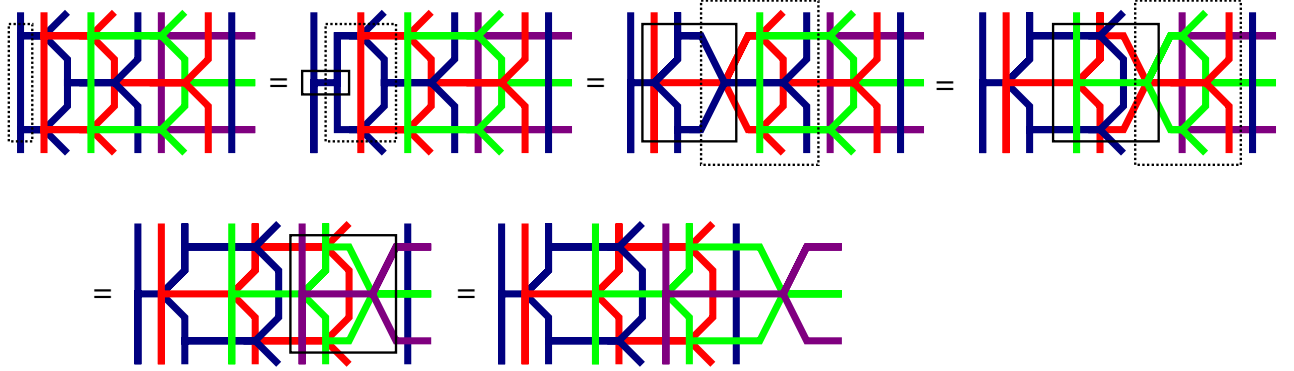
We prove these results for a lift of \mathfrak{s} . The \mathfrak{t} case is analogous.

Proof of (3.20). This is an application of one-color associativity (2.15), and then repeated uses of two-color associativity (2.30), as illustrated in the following example of 3 colors. The dotted rectangle surrounds that which is to be changed, and the solid rectangle what it becomes; the final step is just a distant slide.



Clearly, any calculation for a_3 reduces to this calculation, regardless of the number of total colors in J , because if we choose the expression $s_{J,3}^R$ as the top and bottom of the diagram, then this calculation (tensored on the left with identity maps) will suffice. The calculation clearly generalizes to any number of colors. \square

Proof of (3.21). This is an application of one-color associativity (2.15), then two-color associativity (2.28), then repeated uses of three-color associativity (2.31), as illustrated in the following example of 4 colors.



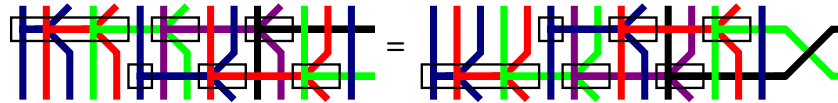
Using the same tricks as the previous proof, we can bootstrap this calculation to deal with any case when teal is i and brown is $i + 1$. \square

In this proof, we repeatedly apply the equality (2.31). If teal and brown were swapped, however, then a similar proof would be forced to use the non-equality (3.1) instead! Unfortunately, when teal and brown are swapped, (3.21) is just false, and one only has the weaker result (3.22).

Note, however, that by applying the Dynkin diagram automorphism to the colors above, one obtains the analogous result for \mathfrak{t} and where teal and brown are swapped.

Proof of (3.22). Use (3.17) to slide each a_i past \bar{Z} , so that they now have top and bottom \mathfrak{t} . Then apply the \mathfrak{t} version of (3.21), and use (3.17) to slide them back. \square

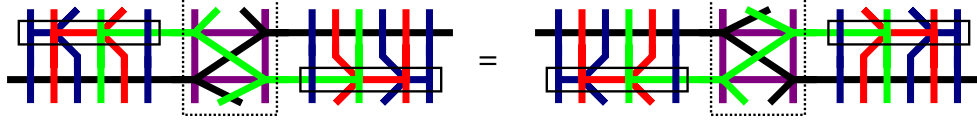
Proof of (3.23). Regardless of which distant colors are chosen, this is a simple application of the distant sliding rules. The reader will observe that any interesting features of a_i will be on strands which are uninteresting in a_j , and vice versa (some strands may be uninteresting for both). This should be clear from the following example.



\square

Proof of (3.24). First, it is important to note that the map a_i^R going to the right and the map a_j^L going to the left require *different* choices of representative of s , either s^R or s^L . To make sense of the equation as, say, endomorphisms of s^R , then one must think of a_j^L as first composing by the distant crossings that bring s^R to s^L , applying a_j as normal, and then applying the distant crossings back. As such, this equation can be a pain to write out in general.

Let us do the hardest case: when $i = j = n$ inside $I = \{1, \dots, n\}$. We will demonstrate the example when $n = 5$. Instead of viewing it as an endomorphism of s^R or s^L , we view it as an endomorphism of 121321435423121 (for the general case, the interesting part in the middle will read $(n-1)(n-2)(n)(n-1)$). Then the reader can observe that the equality may be written suggestively as



This equality follows immediately from three-color associativity (2.31) applied to the dashed box, and distant sliding rules applied to the rest. It should be obvious how this example generalizes to any $n \geq 3$. The cases of $n = 1, 2$ are precisely one-color and two-color associativity.

We leave to the reader the proof that all other cases (for $i < n$ or $j < n$) follow from $i = j = m$ and $J = \{1, \dots, m\}$ for some $m < n$. \square

Proof of (3.25). To prove this, one writes out the map a with a dot, and resolves the dot using (2.26) into a sum of two diagrams. One of the diagrams will die when composed with Z , thanks to Proposition 3.39. The other diagram has a dot attached to another 6-valent vertex, so resolves again using (2.26) into a sum of two diagrams. Again, one of the two will die thanks to Proposition 3.39, and so forth. The single surviving diagram is the identity map. The proof of Lemma 3.44 has a similar argument which is made pictorial. \square

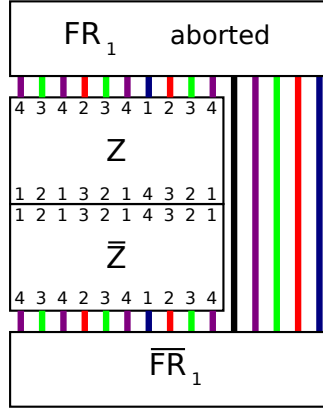
Remark 3.42. There is a direct proof of (3.22) analogous to the proof of (3.25). One adds a new teal-brown 6-valent vertex to both sides of (3.21). The doubled 6-valent vertex on one side can be replaced with the identity, modulo an error term has an aborted 6-valent vertex instead. Resolving this term as in the proof of (3.25), one gets zero.

Similarly, there is an indirect proof of (3.25) similar to the proof of (3.22) and (3.19), which slides a_i past flip maps until it becomes a trivalent vertex, and the dot just pulls in by (2.16).

3.5. Analyzing the path V . The goal of this section is to prove (3.5) along our chosen path V , thereby proving (3.3) and (3.2). Let us restate the goal.

Proposition 3.43. *Let $Q_{\mathbf{x}}$ be the following morphism with bottom boundary \mathbf{s} : one follows the path V , but at some vertex \mathbf{x} along the way, instead of following an adjacent edge $\mathbf{x} \downarrow \mathbf{y}$, one does an aborted 6-valent vertex instead. Then $Q_{\mathbf{x}}\overline{Z} = 0$.*

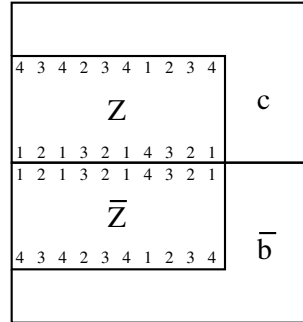
Proof. We prove this statement by induction on the number of colors. The base case of two colors follows from (2.35). So consider the example when $n = 5$, $I = \{1, 2, 3, 4, 5\}$ and $K = \{1, 2, 3, 4\}$. Recall that the path V begins with V_K , and continues with the flip sequence $FR_{\mathbf{t},1}$. If the vertex \mathbf{x} is chosen so that it is part of \overline{V}_K , then $Q_{\mathbf{x}}$ is actually an aborted version of V_K , and $Q_{\mathbf{x}}\overline{Z}$ factors through $Q_{\mathbf{x}}\overline{Z}_K$. Therefore the product is zero by induction. So we may assume that the vertex \mathbf{x} is within the sequence of flips $FR_{\mathbf{t},1}$. Therefore, $Q_{\mathbf{x}}\overline{Z}$ looks like this.



Lemma 3.47 below will show that the aborted version of $FR_{t,1}$ composed with Z_K is a linear combination of certain diagrams, each of which has a dot on one of the strands 54321 which bypass Z_K . Actually, the dot is on one of 5432, and cannot be on the final 1 strand. Lemma 3.46 will show that when this dot is pulled downwards into $\overline{FR}_{t,i}$, it resolves into a linear combination of certain diagrams (actually, the same class of diagrams, upside-down). Finally, Lemma 3.44 will imply that combining any of the diagrams from Lemma 3.47 on top with any of the diagrams from Lemma 3.46 on bottom will yield zero. \square

It remains to describe this class of diagrams which appears, and prove the lemmas.

Lemma 3.44. *(Example: $n = 5$) Let c be one of the pictures in the table of figure 2, and let b be another picture in the same row. For each row, the lines on the right are 54321 except with one index conspicuously absent. The following map is zero, where $z = z_K$ for $K = \{1, 2, 3, 4\}$ and \bar{b} is b upside-down.*



Proof. Note that the leftmost picture in each row is precisely a_i for some i . If both b and c are chosen to be the leftmost picture in a row, then we can use (3.18) to bring the two copies of a_i together, use (3.19) to combine them, and then use (2.17) to show the result is zero. Now we handle the other diagrams in each row by proving that they are obtained from the leftmost by adding a dot on top.

Consider the top row; other rows are entirely analogous. Consider what happens when we place a dot on the leftmost picture in various places. Place a dot on the 3rd to left strand on top (the purple strand) and resolve using relation (2.26). You get two diagrams, one of which is the second diagram on the first row, the other of which factors through a map which vanishes when hit with Z_K , thanks to Proposition 3.39. If you place a dot instead on the 5th strand (green) and resolve, and ignore diagrams which vanish due to Proposition 3.39, then

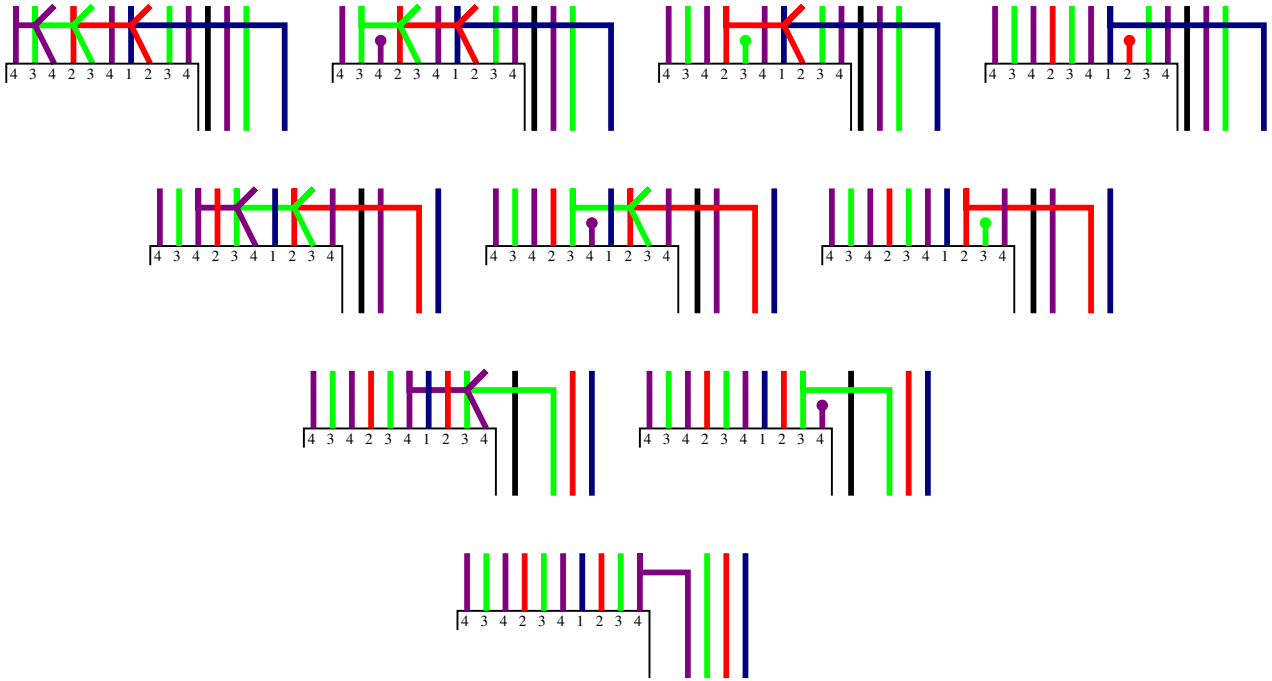
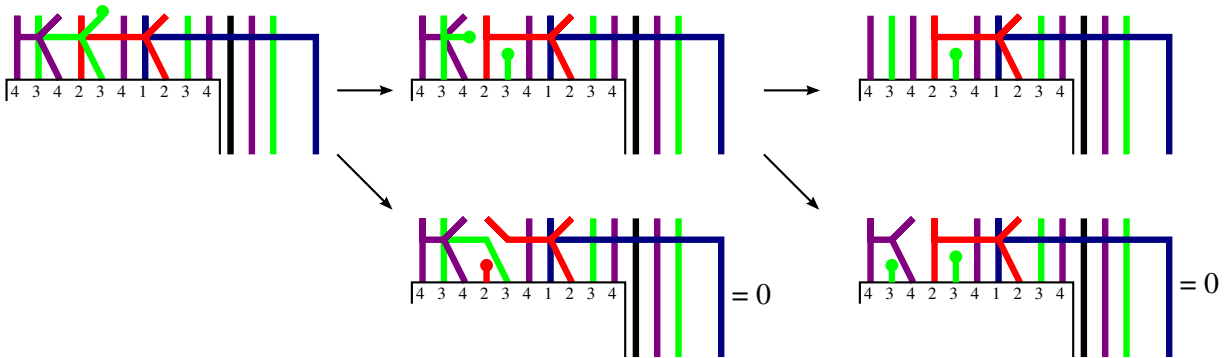


FIGURE 2. Morphisms appearing in Lemmas 3.44 and 3.46

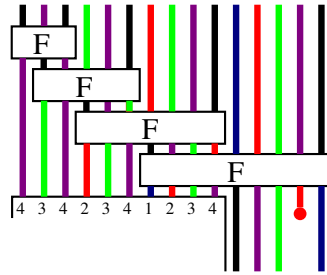
one is left with the third diagram on the first row. Placing a dot on the 8th strand (red) will give the final diagram on that row. \square

Example 3.45. Placing a dot on the 5th strand and resolving:

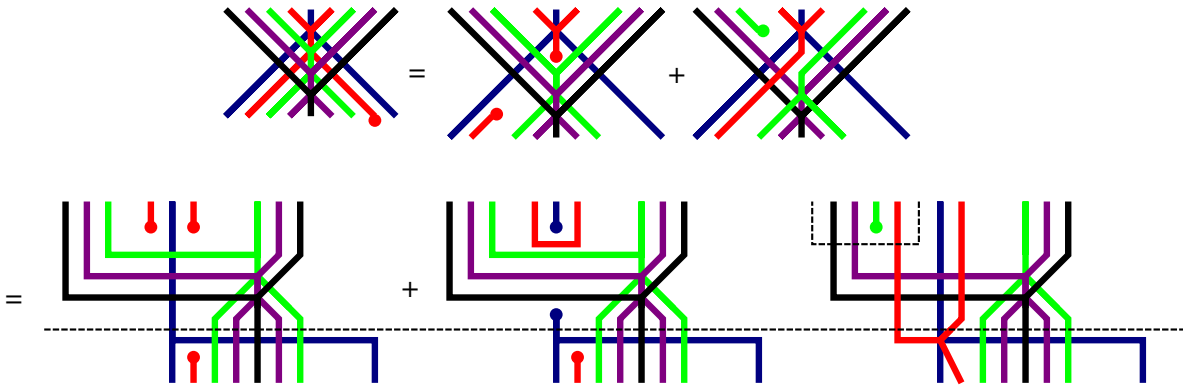


Lemma 3.46. (Example: $n = 5$) Suppose that we place a dot below FR_1 on one of the last strands 54321, but not on the final strand 1. If we place a dot on strand 2, then the resulting morphism can be rewritten as a linear combination of morphisms which factor through the morphisms on the first row of Figure 2. If we place a dot on strand 3, then it can be rewritten to factor through the second row in that figure. Etcetera.

Proof. We shall prove the statement placing a dot on strand 2, and let the reader prove the remainder as an exercise (it follows by the same arguments). The calculation is straightforward but annoying. We are trying to understand the morphism

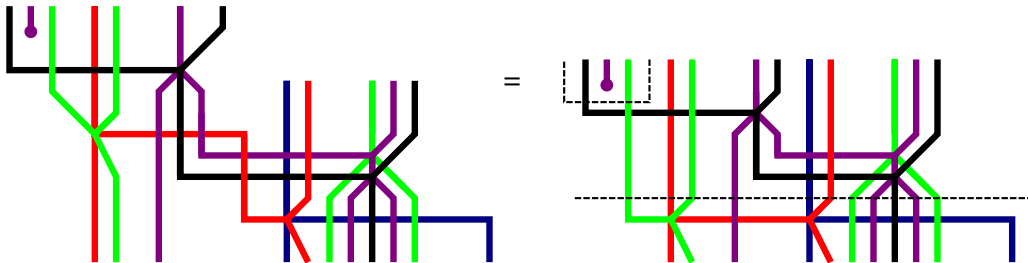


The first step is to resolve the rightmost flip as below, using (2.26) twice.



Having written the final three terms suggestively, we see that the regions below the dotted line are familiar. Note that these diagrams have bottom $1234\ 543\hat{2}1$ with a conspicuously absent 2. Let us compare the part below the dotted line with the part of each diagram in the first row of Figure 2 which only involves $1234\ 543\hat{2}1$. In the first two pictures, the region below the dotted line is precisely the rightmost entry in the first row. Thus we need only deal with the third picture, where the region below the dotted line agrees with the other entries in the first row.

In the third picture, the region enclosed by the dotted box will be passed as input to the next flip map in the sequence. The dot coming into the next flip is green, not red, but it is still the 2nd to right input (which will remain true as we iterate this procedure). Therefore we may resolve the next flip map in the same way, to yield two diagrams which factor through the 2nd to right entry of the first row of Figure 2, and a final diagram which has a dot entering the next flip in the 2nd to right input. The third diagram of this iteration is



Once again, the region below the dotted line agrees with the $234\ 1234\ 543\hat{2}1$ part of the remaining diagrams on the first row of Figure 2. We may then repeat the argument.

Where the argument stops is when the 2nd to right input of a flip is also the central input of a flip. Equivalently, this is when the dot coming into the next flip is black. (If our original dot were on strand 3, we would stop when the 3rd to right input was also the central input of a flip, which is the penultimate flip map.) This black dot enters a black-purple 6-valent vertex. Resolving this using (2.26), we obtain two diagrams, both of which factor through a purple trivalent vertex. This, finally, is the purple trivalent vertex appearing in the first entry of the relevant row of Figure 2. Both diagrams factor through this first entry. \square

Lemma 3.47. *Suppose that we “abort” FR_1 . That is, we follow the path FR_1 from \mathbf{t} up through Γ , but at some vertex \mathbf{x} along the way, instead of following the next adjacent edge $\mathbf{x} \downarrow \mathbf{y}$, we do an aborted 6-valent vertex instead. The resulting morphism then factors through the morphisms in Figure 2, except instead of having a conspicuously absent index on the right, we have a boundary dot instead.*

Example 3.48. Let $n = 5$ and let us abort FR_1 at the top of the bottommost flip $F_{1,5}$. We ignore the sequence of lines 434234 appearing on the left of the morphism. Then using (2.26) repeatedly we resolve as follows.

(3.26)

There are four terms in the end, corresponding to the five indices in 54321 but not counting the final 1. Each term has a dot somewhere in the final string 54321; remove that dot to leave a conspicuously absent strand instead. Each term also has a trivalent vertex or cap (the blue trivalent in the first term, the red cap in the second, the green cap in the third, the purple cap in the fourth) which surrounds the remaining dot, and surrounding a bunch of junk that it slides through. Note that a cap factors through a trivalent vertex, via (2.16). Thus the result factors through the rightmost entry of the appropriate row of Figure 2.

Suppose we had aborted FR_1 inside $F_{1,5}$, but the red-green 6-valent instead of the blue-red 6-valent. This yields a subdiagram of one of the intermediate terms pictured in (3.26) (the rightmost diagram on the top row, replacing the red cap with a red trivalent vertex via (2.16)). In general, aborting $F_{1,5}$ on top, at the blue-red 6-valent vertex, is the hardest; aborting $F_{1,5}$ at any of the other 6-valent vertices and resolving will give subdiagrams of some of the four terms obtained in (3.26). These subdiagrams all factor through the rightmost entry of the appropriate row of Figure 2.

Proof. When we abort FR_1 at the very first edge (the bottommost 6-valent vertex in $F_{1,5}$) we get the bottom entry of Figure 2. Now we use induction on which edge we abort at. As can be seen in the example above, when one aborts and then resolves the dot using (2.26), there are two terms, one of which factors through a previous abortion, and the other of which will provide an interesting new term. This is true also if we abort the first vertex in a new flip,

for we shall have

$$(3.27) \quad \text{Diagram 1} = \text{Diagram 2} + \text{Diagram 3}$$

where the first term is a previous abortion. At each stage, therefore, we will ignore previous abortions by induction. In doing so, we only look at one term in each resolution of (2.26). So we can deterministically replace our aborted copy of FR_1 with another diagram where no dot touches a 6-valent vertex. There are only two operations one needs to perform: replacing the LHS of (3.26) with only the first term on the RHS, and replacing the LHS of (3.27) with only the second term on the RHS.

It is a simple exercise to confirm that this yields precisely the diagrams in Figure 2, with a boundary dot instead of a conspicuously absent strand.

For the example $n = 5$, the path FR_1 has length 10, so there are 10 possible abortions, which we order by the edge aborted. Resolving these modulo previous abortions, we have 10 different diagrams. These factor precisely through the 10 diagrams in Figure 2, in the following order: the rightmost column from bottom to top, then the next rightmost column from bottom to top, and so on. \square

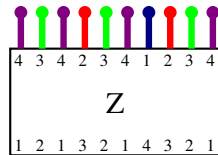
This concludes the proof of Proposition 3.43. Using the arguments of §3.2, we now know that φ_J is a consistent family of projectors.

3.6. Analyzing the image of the projectors. The family φ_J picks out some mutual summand of every reduced expression for w_J , living in the Karoubi envelope of \mathcal{D} , which we temporarily call X . We wish to show that this summand is precisely B_J (we have not even shown yet that X is nonzero).

Proposition 3.49. *The R -bimodule $\text{HOM}_{\mathcal{D}}(X, \emptyset)$ is a free left (or right) R -module of rank 1, generated by the map ξ_J of degree d_J which consists of including X into $B_{\mathbf{x}}$ for some reduced expression \mathbf{x} of w_J , and then placing dots on each strand of $B_{\mathbf{x}}$. This map is independent of the choice of \mathbf{x} .*

Proof. Let $\xi_{\mathbf{t}}$ denote the map $B_{\mathbf{t}} \rightarrow \emptyset$ which puts a dot on every strand. This will descend to a non-zero map from B_J if and only if $\xi_{\mathbf{t}}Z$ is nonzero, since Z is a member of our family φ .

Example 3.50. (Example: $n = 4$) The map ξ :



Consider the functor from diagrammatics to R -bimodules defined in [EK10]. It is easy to see that Z preserves 1-tensors, since the same is true of the 6-valent and 4-valent vertices (we recalled this in §2.3). The collection of dots sends $1 \otimes 1 \otimes \dots \otimes 1$ to 1. Therefore the composition $\xi_{\mathbf{t}}Z$ is nonzero, sending the 1-tensor to 1.

We know that all Hom spaces in SBim are free as left (or right) R -modules, so it is enough to show that every morphism from $B_{\mathbf{t}}$ to \emptyset , when precomposed with Z , reduces to $\xi_{\mathbf{t}}Z$ with some polynomial. If we do this, we will show that the space of morphisms is rank 1, and

therefore is determined by the image of the 1-tensor from $B_{\mathfrak{s}}$. For another $\mathbf{x} \in \Gamma$, letting $\xi_{\mathbf{x}}$ be the collection of dots, the corresponding morphism from B_J is $\xi_{\mathbf{x}}\varphi_{\mathfrak{s},\mathbf{x}}$. But $\varphi_{\mathfrak{s},\mathbf{x}}$ also preserves 1-tensors, so the overall map sends the 1-tensor to 1. Thus, the map is independent of the choice of \mathbf{x} , pending the proof that morphisms are rank 1.

(Example: $n = 4$) We now use the one-color reduction results of [EK10] (and remind the reader to reread this part of [EK10] for some terminology). Consider an arbitrary morphism from $B_{\mathfrak{t}}$ to \emptyset . First simplify the color 1, which is an extremal color (in the Dynkin diagram). Since it appears only once in \mathfrak{t} , we can reduce the 1-colored subgraph to a boundary dot. This boundary dot will not interfere with further simplifications of the diagram. Now consider the color 2, which is an extremal color in the remainder of the morphism. There are exactly two instances of 2 on the boundary, so either they are connected by a line, or they both end in boundary dots. However, if they are connected in a line then the morphism must factor through one of the pictures which vanishes due to Proposition 3.39 (only the last column is needed). So both instances of 2 end in boundary dots, and they will not interfere with further simplification. Now consider the color 3, which is an extremal color in the remainder of the morphism, so it must form a disjoint union of simple trees. There are three instances of 3 on the boundary; call them instance 1, 2, 3. If instance m is connected to instance $m + 1$ in the tree, then the morphism factors through a vanishing picture in Proposition 3.39. If this is not the case, but instance m is connected to instance $m + 2$ (in this case, the only possibility is instance 1 connected to instance 3) then instance 2 ends in a dot. However, we know that

$2 \begin{array}{c} \diagup \quad \diagdown \\ | \\ \bullet \end{array} = \begin{array}{c} \diagup \quad \diagdown \\ \diagdown \quad \diagup \\ | \\ \bullet \end{array} + \begin{array}{c} \diagup \quad \diagdown \\ \diagup \quad \diagdown \\ | \\ \bullet \end{array}$

thanks to (2.18). Therefore, such a morphism factors through one where m and $m + 1$ are connected, for some m , and vanishes by the above arguments. Thus none of the instances are connected, and they must all end in boundary dots. (If one does not believe that morphisms must be free \mathbb{Z} -modules and is worried about 2-torsion, one can calculate that this morphism is zero more directly, without using the (2.18) trick.) Similarly, considering the color 4, no two instances of 4 on the boundary may be connected, since such a morphism will factor through a morphism where instances m and $m + 1$ are connected, and this morphism will vanish thanks to Proposition 3.39. Therefore, any morphism which pairs against Z to be nonzero can be assumed to be $\xi_{\mathfrak{t}}$. \square

Proposition 3.51. *For any $i \in J$, $X \otimes i \cong X(1) \oplus X(-1)$.*

Proof. Note that

$$\begin{aligned}
 \boxed{J} \quad | &= \begin{array}{|c|} \hline J \\ \hline a_i \\ \hline J \\ \hline \end{array} | = \frac{1}{2} \left(\begin{array}{|c|} \hline J \\ \hline a_i \\ \hline J \\ \hline \end{array} \begin{array}{|c|} \hline | \\ \hline | \\ \hline | \\ \hline \end{array} + \begin{array}{|c|} \hline J \\ \hline a_i \\ \hline J \\ \hline \end{array} \begin{array}{|c|} \hline | \\ \hline | \\ \hline | \\ \hline \end{array} \right) \\
 &= \frac{1}{2} \left(\begin{array}{|c|} \hline J \\ \hline a_i \\ \hline J \\ \hline a_i \\ \hline J \\ \hline \end{array} \begin{array}{|c|} \hline | \\ \hline \end{array} + \begin{array}{|c|} \hline J \\ \hline a_i \\ \hline J \\ \hline a_i \\ \hline J \\ \hline \end{array} \begin{array}{|c|} \hline | \\ \hline \end{array} \right)
 \end{aligned}$$

In this calculation, the box labeled J just represents some appropriate projector for X . This calculation, proven using Proposition 3.41, decomposes the identity of $X \otimes i$ into two orthogonal idempotents, in a similar fashion to (2.19). Checking that they are orthogonal idempotents is also easy with Proposition 3.41. \square

Putting these propositions together, we have now proven Theorem 3.18, as outlined in §3.2.

4. THICK CALCULUS

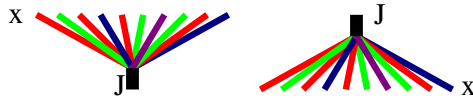
Recall some notation: when J is a connected parabolic subset, W_J is its parabolic subgroup, w_J is the longest element of W_J , and $\tilde{\Gamma}_{w_J}$ is the set of reduced expressions for w_J . The length of w_J is d_J .

In the previous chapter we constructed a family of maps $\varphi_J = \{\varphi_{\mathbf{x},\mathbf{y}}\}$ in \mathcal{D} associated to pairs $\mathbf{x}, \mathbf{y} \in \tilde{\Gamma}_{w_J}$, when J is connected. We proved in Theorem 3.18 that these maps formed a compatible system of projectors, in the sense of Definition 2.13. Thus they pick out a single summand in the Karoubi envelope of \mathcal{D} , a summand we abusively call J . We may now use Claim 2.11 to extend the graphical calculus for \mathcal{D} into a graphical calculus for $g\mathcal{D}$, the partial idempotent completion which adds the new object J for each connected parabolic subset. We have also shown in Theorem 3.18 that the functor from \mathcal{D} to $\mathbb{B}\mathcal{S}\mathcal{B}\text{im}$, extended to the Karoubi envelopes, sends J to B_J . Thus $g\mathcal{D}$ and $g\mathbb{B}\mathcal{S}\mathcal{B}\text{im}$ are equivalent.

Definition 4.1. Let $g\mathcal{D}$ be the graded monoidal category presented diagrammatically as follows. Objects are sequences $\mathbf{J} = J_1 J_2 \dots J_d$ of connected subsets of $I = \{1, \dots, n\}$. When $J = \{j\}$ is a single element, we write the element j instead of writing J , and identify it with an object in \mathcal{D} . We draw the identity of J as follows:



The generating morphisms are the usual generators of \mathcal{D} , in addition to J -inclusions and J -projections. The J -inclusion is a map from J to \mathbf{x} where \mathbf{x} is any reduced expression for w_J . The J -projection is a map in the other direction. Both have degree 0.



The relations are those relations of \mathcal{D} as well as

$$(4.1) \quad \begin{array}{c} \text{Diagram 1} \\ \text{Diagram 2} \end{array} = \begin{array}{c} \text{Diagram 3} \\ \text{Diagram 4} \end{array} .$$

Theorem 4.2. *This diagrammatic category is equivalent to the partial idempotent completion of \mathcal{D} by the images of φ_J . The functor \mathcal{F} from \mathcal{D} to $\mathbb{B}SBim$ extends to a functor from $g\mathcal{D}$ to $g\mathbb{B}SBim$, which is an equivalence when \mathcal{F} is an equivalence.*

Proof. As discussed above, this follows from Claim 2.11 and Theorem 3.18. □

Let us mention where the functor from diagrams to bimodules sends the J -inclusions and J -projections. These are degree zero maps, determined uniquely up to an invertible scalar. We choose the scalars so that the J -projection map sends $1 \otimes 1 \otimes \dots \otimes 1 \in B_x$ to $1 \otimes 1 \in B_J$ for any \mathbf{x} , and so that the J -inclusion map sends $1 \otimes 1 \in B_J$ to $1 \otimes 1 \otimes \dots \otimes 1 \in B_x$. Since the transition maps $\varphi_{\mathbf{x},\mathbf{y}}$ send 1-tensors to 1-tensors, this system of scalars is consistent and the functor is well-defined.

Note that the image of B_J in B_x is spanned by tensors of the form $f \otimes 1 \otimes 1 \otimes \dots \otimes 1 \otimes g$, which we call *extremal tensors*. In other words, the image is generated as a bimodule by the 1-tensor. Since any transition map $\varphi_{\mathbf{x},\mathbf{y}}$ factors through B_J , it must send arbitrary tensors to extremal tensors. To determine what the J -projection map will do to an arbitrary tensor $f_1 \otimes f_2 \otimes \dots \otimes f_d$, we may apply any transition map $\varphi_{\mathbf{x},\mathbf{y}}$ (which is explicit, albeit annoying to compute) to obtain an extremal tensor, and then map the extremal tensor to B_J by the rule $f \otimes 1 \otimes \dots \otimes 1 \otimes g \mapsto f \otimes g$. However, we have not produced anything resembling a closed formula for the J -projection.

We have proven in Proposition 3.24 that, composing $\varphi_{\mathbf{x},\mathbf{y}}$ with a 6-valent or 4-valent vertex $\mathbf{y} \rightarrow \mathbf{z}$ produces $\varphi_{\mathbf{x},\mathbf{z}}$. The implications in $g\mathcal{D}$ are the following two relations.

$$(4.2) \quad \begin{array}{c} \text{Diagram 5} \\ \text{Diagram 6} \end{array} = \begin{array}{c} \text{Diagram 7} \\ \text{Diagram 8} \end{array}$$

$$(4.3) \quad \begin{array}{c} \text{Diagram 9} \\ \text{Diagram 10} \end{array} = \begin{array}{c} \text{Diagram 11} \\ \text{Diagram 12} \end{array}$$

Recall that $\varphi_{\mathbf{x},\mathbf{y}}$ is constructed only out of 4-valent and 6-valent vertices, so that it also “sucks in” to the J -inclusion, a fact which we also know from (4.1). Another implication is that a J -inclusion is orthogonal to an aborted 6-valent vertex, or any of the diagrams in Proposition 3.39 which kill the morphism Z .

As discussed in §2.4, the diagrammatic calculus for $g\mathcal{D}$ can be improved by introducing new pictures which represent maps that can already be obtained from the generators above. This “augmentation” of the diagrammatics makes many statements more intuitive. We now introduce new pictures one at a time with their defining relation, and discuss their properties.

Any relations between these new pictures must be checked in \mathcal{D} using the relations already mentioned. This can be done explicitly, using the calculations of §3 or analogous computations. Some of these checks are huge pains in the neck though. Thankfully, Theorem 4.2 implies that we already know the graded dimension of Hom spaces between objects in $g\mathbb{B}SBim$, and we have a functor to R -bimodules. Thus, if we have two different pictures which represent a map of a certain degree, and the dimension of the Hom space in that degree is 1, then they are equal up to a scalar, and the scalar may often be quickly checked by looking at what the map does to a 1-tensor. This saves a great deal of work.

When calculating these graded dimensions, just remember that $\varepsilon(b_J) = v^{d_J}$, $b_J^2 = [J]b_J$, and $b_J b_i = [2]b_J$ when $i \in J$. For instance, $END(B_J)$ has graded dimension $v^{d_J} [J]$, so it has a 1-dimensional space of degree 0 morphisms, generated by the identity map.

Definition 4.3. The *thick cup* and *thick cap* express the biadjointness of J with itself.

$$(4.4) \quad \text{cup} = \text{thick cup} \quad \text{cap} = \text{thick cap}$$

Thanks to the self-biadjointness of B_i , we know that $B_{\underline{i}}$ is biadjoint to $B_{\omega(\underline{i})}$ (recall that ω reverses the order of a sequence). Consequently, B_v is biadjoint to $B_{v^{-1}}$ for an arbitrary element $v \in W$. The longest element w_J of a parabolic subgroup is an involution, so B_J should be self-biadjoint. The thick cups and caps realize this biadjunction. Note that the thick cups and caps are well-defined because for any reduced expression \mathbf{x} of w_J , $\omega(\mathbf{x})$ is also a reduced expression for w_J . It is straightforward to check the biadjointness relation directly.

$$(4.5) \quad \text{thick dot} = \text{vertical line} = \text{thick dot}$$

Definition 4.4. The *thick dot* is obtained by choosing a reduced expression \mathbf{x} for w_J and composing $J \rightarrow \mathbf{x} \rightarrow \emptyset$, where the latter map consists of a dot on every strand.

$$(4.6) \quad \text{thick dot} = \text{thick dot with colored strands}$$

This was the map called ξ_J in Proposition 3.49. From that proposition we have:

Claim 4.5. *The map above is nonzero, and independent of the choice of x , so it is well defined. It is the generator of $\text{Hom}_{g\mathcal{D}}(J, \emptyset)$ as an R -bimodule.*

The definition of an upside-down thick dot is the same, only flipped upside-down. The cyclicity of thick dots is quite clear.

$$(4.7) \quad \text{upside-down thick dot} = \text{thick dot} = \text{upside-down thick dot}$$

Definition 4.6. The *thick crossing* exists only when J and K are *distant*, that is, every index inside them is distant. It agrees with the usual 4-valent crossing when $J = \{j\}$ and $K = \{k\}$.

(4.8)

This crossing gives the isomorphism $J \otimes K \cong K \otimes J$ for J, K distant. There will be distant sliding rules, which we will present in full after all the new pictures have been presented. Once again, it is obvious that the thick crossing is cyclic.

(4.9)

Definition 4.7. The *thick trivalent vertex* exists only when $i \in J$. It agrees with the usual trivalent vertex when J is a singleton. Thick trivalent vertices may be *right-facing* as in the picture below, or may be *left-facing* (sending the extra index i off to the left). For the definition of a_i , see §3.4.

(4.10)

The utility of these maps has already been seen in the proofs of the previous section. These relations rephrase Proposition 3.41.

(4.11)

(4.12)

(4.13)

(4.14)

(4.15) 

Note that (4.13) only makes sense when the teal and brown indices are adjacent, and (4.14) only when they are distant.

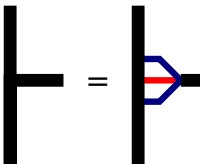
In addition, a quick comparison of a_i when expressed on the right for s_J^R and on the left for t_J^L will convince the reader of the cyclicity of the thick trivalent vertex.

(4.16) 

Rephrasing the isomorphism $B_J \otimes B_i \cong [2] B_J$ in terms of thick trivalent vertices is easy given from Proposition 3.51. We leave it to the reader to prove that the thick trivalent vertex, viewed as a morphism $J \otimes i \rightarrow J$, is the unique morphism of degree -1 up to scalar, and after applying the functor to bimodules, it sends $f \otimes g \otimes h \mapsto f \otimes \partial_i(g)h$. (Hint: use a reduced expression for w_J ending in i .)

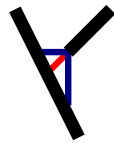
Now, we wish to give a diagrammatic relation corresponding to the isomorphism $B_J \otimes B_J \cong [J] B_J$, and so we will need a number of projection and inclusion maps between $B_J \otimes B_J$ and B_J of various different degrees. We construct these in a fashion entirely akin to the isomorphism $B_i \otimes B_i \cong [2] B_i$. First, we find the projection/inclusion of minimal degree, and draw it as a trivalent vertex.

Definition 4.8. The *very thick trivalent vertex* is constructed as follows. Rotate the J -inclusion for \mathbf{x} by 90 degrees, and then connect the output sequence \mathbf{x} to another J -colored strand by a sequence of thick trivalent vertices. There are d_J thick trivalent vertices, so this morphism has degree $-d_J$.

(4.17) 

This map does not depend on the choice of \mathbf{x} . If we combine (4.13) with (4.2), or (4.14) with (4.3), we can alter \mathbf{x} by applying any braid relation.

Moreover, it is true, but not immediately obvious, that the morphism is cyclic. We show this via the functor to bimodules. Recall that there is a unique morphism of degree $-d_J$ from $B_J \rightarrow B_J \otimes B_J$ up to scalar, and similarly from $B_J \otimes B_J \rightarrow B_J$. Consider the map

 . It is easy to observe that this map sends the 1-tensor to the 1-tensor, and so does

its horizontal reflection, so the map is equal to its horizontal reflection.

Definition 4.9. Let \underline{i} be a reduced expression of w_J . Then $\partial_{\underline{i}} := \partial_{i_1} \dots \partial_{i_{d_J}}$, the composition of Demazure operators, is independent of the choice of reduced expression. The result is a degree $-2d_J$ map from $R \rightarrow R^J$ which is R^J -linear. It is denoted ∂_J and is also called a *Demazure operator*.

∂_J is the nondegenerate trace, so that there is some set of polynomials $\{g_r\}$ which is a basis for R as an R^J -module (free of graded rank $[J]$), and some other basis $\{g_r^*\}$ as well, for which $\partial_J(g_r g_q^*) = \delta_{r,q}$. These polynomials are indexed by $r \in W_J$, and g_r has degree $2l(r)$, while g_r^* has degree $2(d_J - l(r))$. We may as well assume that $g_1 = g_{w_J}^* = 1$.

Claim 4.10. *The element $\beta = \sum_{W_J} g_r \otimes g_r^* \in B_J$ satisfies $f\beta = \beta f$ for any $f \in R$.*

This is a standard fact about Frobenius algebras. One obtains the same element β regardless of which basis and dual basis we choose. Alternatively, we may define β as the image of $1 \in R$ under the thick dot.

Remark 4.11. In type A, there is a nice choice of basis and dual basis known as *Schubert polynomials*. The advantage of Schubert polynomials in type A is that one may choose other Schubert polynomials to form the dual basis. However, we never make any assumptions about the choice of basis in this paper.

The internet contains numerous easily-obtained resources on Frobenius algebras and Schubert polynomials.

As discussed above, the very thick trivalent vertex, seen as a map from $R \otimes_{R^J} R \otimes_{R^J} R \{-2d_J\} = B_J \otimes B_J \rightarrow B_J$, applies the Demazure operator ∂_J to the middle term, while seen as a map from $B_J \rightarrow B_J \otimes B_J$, it adds 1 as the middle term. We now list some relations which can be deduced from the previous discussion without too much effort, and are obvious generalizations of the one-color relations for \mathcal{D} . Recall that a box with $f \in R$ inside represents multiplication by f .

$$(4.23) \quad \begin{array}{c} \text{thick trivalent vertex with } [f] \text{ in the middle} \end{array} = \begin{array}{c} \text{thick vertical line} \text{ with } \boxed{\partial_J(f)} \text{ on the right} \end{array}$$

$$(4.24) \quad \begin{array}{c} \text{thick vertical line with two dots} \end{array} = \sum \begin{array}{c} \boxed{g_r} \text{ on the left, } \boxed{g_r^*} \text{ on the right} \end{array}$$

$$(4.25) \quad \begin{array}{c} \text{two thick vertical lines} \end{array} = \sum \begin{array}{c} \text{thick trivalent vertex with } \boxed{g_r} \text{ on top and } \boxed{g_r^*} \text{ on bottom} \end{array}$$

The last relation expresses the decomposition $B_J \otimes B_J \cong [J] B_J$.

We make one further extension of the calculus.

Definition 4.12. The *generalized thick trivalent vertex*, with top and bottom boundary J and right boundary K for $K \subset J$, is constructed in the same fashion as the very thick trivalent

vertex, and generalizes both the very thick trivalent vertex and the thick trivalent vertex.

$$(4.26) \quad \begin{array}{c} J \\ | \\ \text{---} K \\ | \\ J \end{array} = \begin{array}{c} J \\ | \\ \text{---} K \\ | \\ J \end{array}$$

The reader should easily be able to generalize the previous discussion to this new picture. In particular, it is cyclic, satisfies various associativity properties akin to (4.12) and (4.15), a unit axiom akin to (4.20) or (4.11), and another one akin to (4.22). It has distant sliding rules, applies the Demazure operator ∂_K to the middle term in $B_J \otimes B_K$, and can be used to express the isomorphism $J \otimes K \cong [K]J$.

Remark 4.13. In fact, the category $g\mathcal{D}$ is generated entirely by generalized thick trivalent vertices, thick dots, and thick crossings. It is not too hard to see that the other maps in $g\mathcal{D}$, namely the 6-valent vertex and the J -projections and J -inclusions, can actually be constructed out of these. Below, the thick line represents $J = \{1, 2\}$.

There are presumably many more interesting relations to be found, but these shall be good enough for now. Finding the relations which intertwine thick lines in interesting ways is a more difficult problem.

Remark 4.14. We have chosen to define thick strands only for connected parabolic subsets J . Suppose J is a *disconnected* parabolic subset, so $J = J_1 \amalg \cdots \amalg J_k$ for connected, mutually distant parabolic subsets J_i . Thus $W_J = W_{J_1} \times \cdots \times W_{J_k}$, w_J is the product of the various w_{J_i} , and B_J is the tensor product of the B_{J_i} in $\mathbb{S}\text{Bim}$. So the object B_J is already isomorphic to an object in $g\mathcal{D}$.

However, if we wished, we could extend the diagrammatic calculus to include thick lines labeled by disconnected parabolic subsets J . In fact, all the diagrammatic conventions and relations above work verbatim in this context, once one defines the morphism a_i correctly. If we let \mathbf{s}_J (the source in the graph Γ_{w_J}) be the concatenation of \mathbf{s}_{J_i} (and the same for \mathbf{t}), then we may view the path morphism from $\mathbf{s}_J \rightarrow \mathbf{t}_J$ diagrammatically as the horizontal concatenations of the path morphism for each component. To define a_i for J , define it for the connected subgraph of which i is a part, and then extend it via the identity map to the remainder of J , possibly crossing the sideways i -strand across various distant identity maps. Thanks to distant sliding rules, this a_i has all the desired properties. Theorem 3.18 is easily adapted to disconnected J as well.

5. INDUCED TRIVIAL REPRESENTATIONS

Recall from Sections 2.1 and 2.2 that the induced (left) representation T_J is the left ideal generated by b_J in \mathbf{H} . To categorify this, we wish to use the “left ideal” generated by B_J in $g\mathbb{S}\text{Bim}$, or in the smaller partial idempotent completion $\mathbb{S}\text{Bim}(B_J)$. The diagrammatic version of this ideal in $g\mathcal{D}$ would be all pictures which have a thick line labelled J appearing on the right. However, because we will eventually take idempotent completions, the source and target of our diagram may be assumed to be an object in \mathcal{D} tensored with J . We may as well let the remainder of the diagram be a picture in \mathcal{D} , and view the thick line on the right as some sort of “membrane” which interacts in a specific way with the morphisms in

Claim 5.5. *These functors are well defined, and preserve the (R, R^J) -bimodule structure of Hom spaces. The composition of functors from \mathcal{T}_J to $g\mathcal{D}$ and then to $g\mathbb{B}S\text{Bim}$ is equal to the composition of functors from \mathcal{T}_J to $J\mathbb{B}S\text{Bim}$ and then to $g\mathbb{B}S\text{Bim}$ by inducing from R^J to R .*

Proof. Given the calculations and remarks of the previous chapter, it is entirely straightforward to check this on objects and on generating morphisms. \square

Consider the map $\text{Hom}_{\mathcal{T}_J}(\underline{i}, \underline{j}) \rightarrow \text{Hom}_{g\mathcal{D}}(\underline{i}J, \underline{j}J)$ given by this functor. We will show that this map is an injection. It is not a surjection, essentially because it misses polynomials to the right of the thick line. For example, consider the left side of (4.24). This does not correspond to a map in \mathcal{T}_J from $\emptyset \rightarrow \emptyset$ because it factors in $g\mathcal{D}$ through an object \emptyset without J on the right, so can not be described with a membrane. Thanks to (4.24), however, we may express it as a linear combination of morphisms in the image of \mathcal{T}_J but with added polynomials on the right. This is the only obstruction to being a surjection, that is, there will be an isomorphism

$$(5.3) \quad \text{Hom}_{\mathcal{T}_J}(\underline{i}, \underline{j}) \otimes_{R^J} R \rightarrow \text{Hom}_{g\mathcal{D}}(\underline{i}J, \underline{j}J).$$

Because any polynomial in R^J will slide across a thick J -colored strand, placing this polynomial to the left of the membrane and applying the functor agrees with placing it on the far right of the diagram after applying the functor. Thus this map is well-defined.

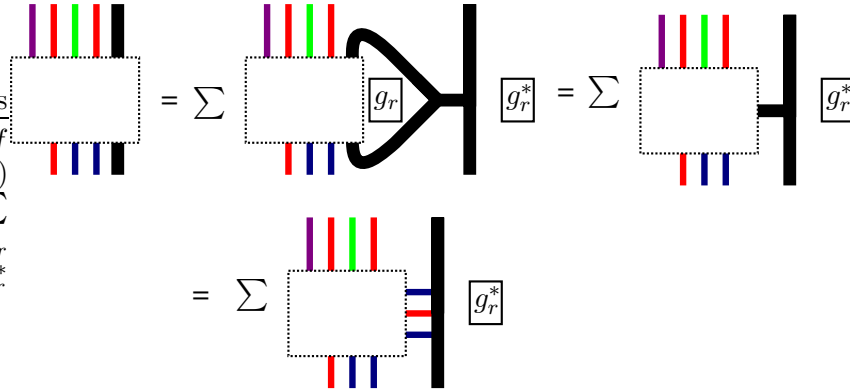
Recall from Section 2.2 that for two $R - R^J$ -bimodules X, Y in $J\mathbb{B}S\text{Bim}$ we have an R -bimodule isomorphism $\text{Hom}_{\mathbb{S}\text{Bim}}(X \otimes_{R^J} R, Y \otimes_{R^J} R) \cong \text{Hom}_{J\mathbb{B}S\text{Bim}}(X, Y) \otimes_{R^J} R$.

Theorem 5.6. *The functor from \mathcal{T}_J to $J\mathbb{B}S\text{Bim}$ is an equivalence of categories.*

Proposition 5.7. *The map in (5.3) is an isomorphism.*

Corollary 5.8. *The space $\text{Hom}_{\mathcal{T}_J}(\underline{i}, \underline{j})$ is a free left R -module of graded rank $v^{-d_J} \varepsilon(b_J b_{\underline{i}} b_{\omega(\underline{j})})$.*

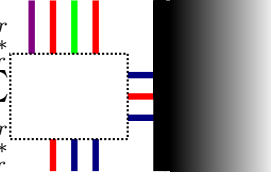
Proof. First we show that the map in (5.3) is surjective. Consider an arbitrary morphism in $g\mathcal{D}$ from $\underline{i}J$ to $\underline{j}J$. We can merge the two J inputs (top right, bottom right) using the relation (4.25).



Then, using the definition in $g\mathcal{D}$ of the very thick trivalent vertex, we may rewrite the equation as above. The lines emanating from the thick line in the final picture form some reduced expression \mathbf{x} of w_J . The morphism inside the box (by which we always refer to the box in the bottom diagram above) may be different in each term of the sum. Note that the morphism inside the box is a morphism between objects in \mathcal{D} , and since \mathcal{D} includes fully faithfully into its partial idempotent completion $g\mathcal{D}$, we may assume that the morphism inside

the box only uses diagrams from \mathcal{D} (i.e. no further thick lines are present). Therefore, every morphism is in the image of (5.3).

In fact, the calculation above implies that $\text{Hom}_{g\mathcal{D}}(\underline{i}J, \underline{j}J)$ is precisely $M \otimes_{R^J} R$, where $M = \text{Hom}_{\mathcal{D}}(\underline{i}\mathbf{x}, \underline{j})\varphi_{\mathbf{x}, \mathbf{x}}$ is the space of all morphisms in \mathcal{D} which fit inside the box, and which are unchanged when composed with the transition map $\varphi_{\mathbf{x}, \mathbf{x}}$ along the \mathbf{x} input. We claim that any morphism in \mathcal{T}_J comes from a diagram in M . The point is that, using (4.11), we can ensure that the sequence of colors which meets the membrane is arbitrarily long, and then using (4.12), (4.13), and (4.14) we can reduce this sequence to any given expression \mathbf{x} for w_J .



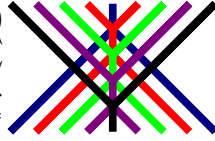
Therefore we have a surjective map $M \rightarrow \text{Hom}_{\mathcal{T}_J}(\underline{i}, \underline{j})$, which provides the inverse of the Hom space map above. This proves the proposition.

Because the various functors compose properly as in Claim 5.5, it would be impossible for the above map to be an isomorphism unless the functor from $\mathcal{T}_J \rightarrow \mathcal{JBSBim}$ is fully faithful. This proves the theorem. Thus, too, is the Corollary proven, since Hom spaces in \mathcal{JBSBim} are free as right or left modules, and graded ranks in \mathcal{JBSBim} are known already to agree with this formula (see the end of Section 2.2). \square

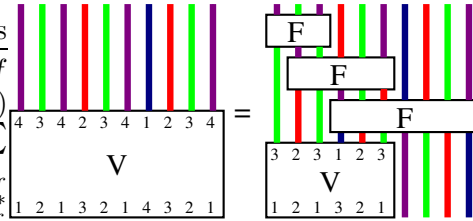
APPENDIX A. SUMMARY OF NOTATION

- W is the symmetric group S_{n+1} . $I = \{1, \dots, n\}$ is the indexing set of simple reflections. w_0 is the longest element.
 - J and K are *parabolic subsets*, subsets of I .
 - W_J is the parabolic subgroup attached to J , with longest element w_J . The length of w_J is d_J . The Poincaré polynomial of W_J is $[J]$.
 - \underline{i} is a sequence of indices in I . $s_{\underline{i}}$ is the corresponding element in W . \underline{J} is a sequence of parabolic subsets.
 - \mathbf{H} is the Hecke algebra of S_{n+1} . \mathbf{H}_J is the subalgebra for W_J .
 - $\{b_w\}$ is the Kazhdan-Lusztig basis of \mathbf{H} . $b_i = b_{s_i}$ and $b_J = b_{w_J}$.
 - T_J is the left ideal of b_J in \mathbf{H} .
-
- R is the polynomial ring in $n+1$ variables f_i , over a base field k . It has an action of W . It is graded, with f_i in degree 2.
 - R^J are the invariants of R under W_J . R^i are the invariants under s_i .
 - HOM denotes the graded vector space of morphisms of all degrees in a graded category.
 - $B_i = R \otimes_{R^i} R(1)$. $B_J = R \otimes_{R^J} R(d_J)$. The grading shift places the *1-tensor* $1 \otimes 1$ in negative degree.
 - $B_{\underline{i}} = B_{i_1} \otimes_R \dots \otimes_R B_{i_d}$. $B_{\underline{J}} = B_{J_1} \otimes_R \dots \otimes_R B_{J_d}$.
 - $\mathbb{B}\text{SBim}$ is the full subcategory of graded R -bimodules with objects $B_{\underline{i}}$. \mathcal{D} is the diagrammatic category which is (usually) equivalent to it.
 - $g\mathbb{B}\text{SBim}$ is the full subcategory of graded R -bimodules with objects $B_{\underline{J}}$. $g\mathcal{D}$ is its diagrammatic version.
 - $J\mathbb{B}\text{SBim}$ is the full subcategory of (R, R^J) -bimodules whose objects are restrictions of $B_{\underline{i}}$. \mathcal{T}_J is the diagrammatic version.
 - $\mathbb{S}\text{Bim}$ is the Karoubi envelope of $\mathbb{B}\text{SBim}$.
 - ∂_i and ∂_w are Demazure operators. See [EK10].
-
- $\tilde{\Gamma}_w$ is the (expanded) graph of all reduced expressions of w . If w is omitted, it is usually w_0 .
 - Γ_w is the conflated graph of reduced expressions.
 - $\mathbf{x}, \mathbf{y}, \mathbf{z}$ are vertices either in $\tilde{\Gamma}_w$ or in Γ_w . In $\tilde{\Gamma}_w$ they are sequences of indices, like \underline{i} , but unlike \underline{i} they are always assumed to be reduced expressions of the element w in question. In Γ_w they are equivalence classes of reduced expressions.
 - $B_{\mathbf{x}}$ is the corresponding object in $\mathbb{B}\text{SBim}$ or in \mathcal{D} . When \mathbf{x} is a vertex in Γ_w , this represents a canonical isomorphism class in \mathcal{D} .
 - $\mathbf{x} \searrow \mathbf{y}$ is some oriented path in $\tilde{\Gamma}_w$ or Γ_w . $\mathbf{x} \downarrow \mathbf{y}$ is a single oriented edge in Γ_w . $\psi_{\mathbf{x} \searrow \mathbf{y}}$ is the corresponding path morphism.
 - The *aborted 6-valent vertex* is the map (2.34), which has the same source as a 6-valent vertex, and can be placed in its stead in the *aborted* version of a path morphism.
 - \overline{D} is the path D in reverse, or the diagram D turned upside-down.
-
- \mathbf{s} is the unique source in Γ_{w_0} . \mathbf{t} is the unique sink.
 - Anything with subscript J is the corresponding thing for Γ_{w_J} for a connected parabolic subset J .
 - $Z = \psi_{\mathbf{s} \searrow \mathbf{t}}$.
 - $\varphi_{\mathbf{x}, \mathbf{y}}$ corresponds to the path $\mathbf{x} \searrow \mathbf{t} \nearrow \mathbf{s} \searrow \mathbf{y}$.

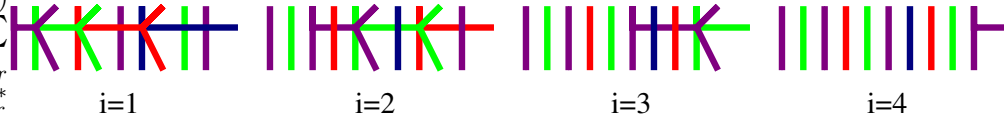
- $\chi_{\mathbf{x},\mathbf{y}}$ corresponds to the path $\mathbf{x} \nearrow \mathbf{s} \searrow \mathbf{t} \nearrow \mathbf{y}$.
- Color conventions: blue red green purple black is 12345.
- $n = 5$: $\mathbf{s}^R = 1\ 21\ 321\ 4321\ 54321$. $\mathbf{t}^R = 5\ 45\ 345\ 2345\ 12345$.
- $n = 5$: $\mathbf{s}_3^R = 12345\ 1234\ 1\ 21\ 321$. It ends in $\mathbf{s}_{\{1,2,3\}}^R$. $\mathbf{t}_3^R = 54321\ 5432\ 5\ 45\ 345$. It ends in $\mathbf{t}_{\{3,4,5\}}^R$.
- $F_{1,5}$ is the *flip*, a path $123454321 \searrow 543212345$.



- $FR_{\mathbf{t},i}$ is a particular sequence of flips, which ends in \mathbf{t} , and whose source has i on the right.
- $FR_{\mathbf{s},i}$ starts at \mathbf{s} , and ends with i on the right.
- V is a particular path from \mathbf{s}^R to \mathbf{t}^R , built inductively. $FR_{\mathbf{t},1}$ is the sequence of flips above the smaller V .



- Color conventions: teal and brown are arbitrary indices in J .
- $a_i = a_{\mathbf{x},i}^R$ is a particular diagram with top and bottom boundary \mathbf{x} and side boundary i on the right. It is only defined explicitly for $\mathbf{x} = \mathbf{s}$ or $\mathbf{x} = \mathbf{t}$. Here is $a_{\mathbf{t}^R,i}^R$.



- ξ_J is a map from B_J or $B_{\mathbf{x}}$ to \emptyset , which puts a dot on every strand.

REFERENCES

- [BNM06] Dror Bar-Natan and Scott Morrison. The Karoubi envelope and Lee’s degeneration of Khovanov homology. *Algebr. Geom. Topol.*, 6:1459–1469, 2006.
- [CKM14] Sabin Cautis, Joel Kamnitzer, and Scott Morrison. Webs and quantum skew Howe duality. *Math. Ann.*, 360(1-2):351–390, 2014.
- [EK10] Ben Elias and Mikhail Khovanov. Diagrammatics for Soergel categories. *Int. J. Math. Math. Sci.*, pages Art. ID 978635, 58, 2010.
- [Eli10] Ben Elias. A diagrammatic Temperley-Lieb categorification. *Int. J. Math. Math. Sci.*, pages Art. ID 530808, 47, 2010.
- [EW] Ben Elias and Geordie Williamson. Soergel calculus. Preprint. arXiv:1309.0865.
- [EW14] Ben Elias and Geordie Williamson. The Hodge theory of Soergel bimodules. *Ann. of Math. (2)*, 180(3):1089–1136, 2014.
- [Kau87] Louis H. Kauffman. State models and the Jones polynomial. *Topology*, 26(3):395–407, 1987.
- [KL09] Mikhail Khovanov and Aaron D. Lauda. A diagrammatic approach to categorification of quantum groups. I. *Represent. Theory*, 13:309–347, 2009.
- [KL11] Mikhail Khovanov and Aaron D. Lauda. A diagrammatic approach to categorification of quantum groups II. *Trans. Amer. Math. Soc.*, 363(5):2685–2700, 2011.
- [KLMS12] Mikhail Khovanov, Aaron D. Lauda, Marco Mackaay, and Marko Stošić. Extended graphical calculus for categorified quantum $\mathfrak{sl}(2)$. *Mem. Amer. Math. Soc.*, 219(1029):vi+87, 2012.
- [Kup96] Greg Kuperberg. Spiders for rank 2 Lie algebras. *Comm. Math. Phys.*, 180(1):109–151, 1996.
- [Lau10] Aaron D. Lauda. A categorification of quantum $\mathfrak{sl}(2)$. *Adv. Math.*, 225(6):3327–3424, 2010.
- [Lib08] Nicolas Libedinsky. Sur la catégorie des bimodules de Soergel. *J. Algebra*, 320(7):2675–2694, 2008.
- [Lib11] Nicolas Libedinsky. New bases of some Hecke algebras via Soergel bimodules. *Adv. Math.*, 228(2):1043–1067, 2011.
- [Lus14] George Lusztig. Hecke algebras with unequal parameters. Revision, 2014. arXiv:0208154v2.
- [MS89] Yu. I. Manin and V. V. Schechtman. Arrangements of hyperplanes, higher braid groups and higher Bruhat orders. In *Algebraic number theory*, volume 17 of *Adv. Stud. Pure Math.*, pages 289–308. Academic Press, Boston, MA, 1989.
- [MS08] Volodymyr Mazorchuk and Catharina Stroppel. Categorification of (induced) cell modules and the rough structure of generalised Verma modules. *Adv. Math.*, 219(4):1363–1426, 2008.
- [Rou08] Raphaël Rouquier. 2-Kac-Moody algebras. Preprint, 2008. arXiv:0812.5023.
- [SAV15] Seth Shelley-Abrahamson and Suhas Vijaykumar. Higher Bruhat orders in type B. Preprint, 2015. arXiv 1506.05503.
- [Soe90] Wolfgang Soergel. Kategorie \mathcal{O} , perverse Garben und Moduln über den Koinvarianten zur Weylgruppe. *J. Amer. Math. Soc.*, 3(2):421–445, 1990.
- [Soe92] Wolfgang Soergel. The combinatorics of Harish-Chandra bimodules. *J. Reine Angew. Math.*, 429:49–74, 1992.
- [Soe07] Wolfgang Soergel. Kazhdan-Lusztig-Polynome und unzerlegbare Bimoduln über Polynomringen. *J. Inst. Math. Jussieu*, 6(3):501–525, 2007.
- [Sto11] Marko Stosic. Indecomposable 1-morphisms of \dot{U}_3^+ and the canonical basis of $U_q^+(\mathfrak{sl}_3)$. Preprint, 2011. arXiv:1105.4458.
- [VV11] M. Varagnolo and E. Vasserot. Canonical bases and KLR-algebras. *J. Reine Angew. Math.*, 659:67–100, 2011.
- [Wil11] Geordie Williamson. Singular Soergel bimodules. *Int. Math. Res. Not. IMRN*, (20):4555–4632, 2011.
- [Wil13] Geordie Williamson. Schubert calculus and torsion. Preprint, 2013. arXiv:1309.5055.

Ben Elias, Department of Mathematics, University of Oregon, Eugene, OR 97403
 email: belias@uoregon.edu